JCHS

TU Delft OPEN

JOURNAL OF COASTAL AND HYDRAULIC STRUCTURES

Vol. 2, 2022, 13

Loads and effects of ship-generated, drawdown waves in confined waterways - A review of current knowledge and methods

León-Carlos Dempwolff[1], Gregor Melling[2], Christian Windt[1], Oliver Lojek[1], Tobias Martin[3], Ingrid Holzwarth[2], Hans Bihs[3], Nils Goseberg[1,4]

Abstract

A ship in motion generates a complex wave field consisting of several superimposed wave systems. The relevance of the wave systems' components varies, depending on individual ship and waterway parameters. This review work is specifically concerned with the long-period, primary wave system, generated by large-volume ships travelling through confined waterways. This wave system may exert intensive wave and current loading on the banks, affecting local morphology, engineering structures and ecology.

The ship-induced loading has recently become more relevant, since ship sizes increase and traffic intensifies, leading to higher and more frequent loads. Especially in non-homogeneous waterways, like estuaries and natural or re-naturalized rivers, shallow-water wave deformation processes affect the far field loading induced by ships. Thus, methods to predict these loads need to account for site-specific effects regarding wave generation and propagation.

This review paper compiles, analyzes, and assesses the findings of previous research quantifying the relevance of primary waves for the surrounding waterways and shows interconnections to the questions studied within naval hydrodynamics for confined waterways. Commonly applied methods for wave prediction are reviewed, highlighting their relevance and limitations. Finally, a concept for coupled numerical model development is suggested, based on the success of different modelling approaches presented previously.

Keywords:

Ship-generated waves, primary-wave system, confined waterways, wave loading, environmental impact

[1]l.dempwolff@tu-braunschweig.de, c.windt@tu-braunschweig.de, o.lojek@tu-braunschweig.de, n.goseberg@tu-braunschweig.de; Technische Universität Braunschweig, Germany
[2]gregor.melling@baw.de, ingrid.holzwarth@baw.de; Federal Waterways Engineering and Research Institute (BAW), Hamburg, Germany
[3]tobias.martin@ntnu.no, hans.bihs@ntnu.no; Norwegian University of Science and Technology (NTNU), Trondheim, Norway
[4]goseberg@fzk.uni-hannover.de; Coastal Research Center, Hannover, Germany

This paper was submitted on May 21, 2021. It was accepted after double-blind review on March 7, 2022 and published online on May 10, 2022.

DOI: https://doi.org/10.48438/jchs.2022.0013

Cite as: Dempwolff, L.-C., Melling, G., Windt, C., Lojek, O., Martin, T., Holzwarth, I., Bihs, H., Goseberg, N. (2022). Loads and effects of ship-generated, drawdown waves in confined waterways - A review of current knowledge and methods, Journal of Coastal and Hydraulic Structures, 2. https://doi.org/10.48438/jchs.2022.0013

1 Introduction

In the last decades, the fleet of marine and inland vessels travelling waterways has significantly evolved. An increasing amount of goods is transported on international sea routes, driven by the developments in a globalized economy. As a result of cost optimization, larger ships are employed, increasing the transport capacity per ship. The average capacity of container ships almost quadrupled between 1990 and 2016, while the average capacity of newly built container ships increased by a factor of six in the same period (Haralambides, 2017). The maximum capacity of the currently largest ship, the HMM Algeciras, is 24,000 Twenty-foot equivalent Unit (TEU) (Marine Insight, 2021). These ships often need to travel through confined waterways, limited either in lateral extent (navigable width) or water depth, to access sea or estuarine ports. It is well known that in confined waterways the hydrodynamic processes induced by a ship result in a bilateral influence between the ship and the waterway.

The dynamic behaviour of ships in confined waterways has been studied intensively under the aspect of safe and efficient navigation. In many confined waterways, ship-generated waves and associated currents have been reported to exert significant loads on the environment, i.e. embankments, pluvial plains, mudflats, and cut-off meanders, to just name a few of the relevant coastal, estuarine, and riverine water body features. The wave field generated by a ship is known to be complex and comprises different components of varying relevance, dependent on ship speed and dimensions, as well as the waterway bathymetry. Case studies highlight the varying relevance of the respective wave components depending on the local traffic and naturally occurring loads at specific sites. Literature reporting on damage induced by ship waves and case studies will be further analyzed within this article.

Large ships, as used for commercial purposes nowadays, generate primary waves of significant magnitude when travelling through confined waterways. While smaller vessels also generate primary wave systems, they are generally less impactful, and the authors have deliberately limit themselves to the effects of larger vessels. These waves, characterized by their long period, exhibit different load parameters on the water bodies' perimeter than other ship-generated wave systems. Even though the physical phenomenon has been known for a long time, the need to further quantify waves generated by ships and their effects is a consequence of their increasing size. Throughout the last decades, various researchers specifically report on damaging influences of primary ship waves in different locations around the world and suggest different strategies to predict them. The literature we identified originates from various disciplines, as the examination of the complex and multi-faceted processes is of interest to researchers from a range of scientific fields, comprising naval architecture, applied maths, river ecology, as well as river, estuarine and coastal engineering. This work hence seeks to highlight the interconnections between the various research questions posed, present the methods used in different scientific disciplines and to promote further interdisciplinary cooperation in addressing them. In addition, long-standing, previously unpublished research results from the Elbe river, are introduced, focusing on damaged groins in the light of primary ship waves.

Several review papers, looking into ship-generated waves and their impacts, have been published in the past. Soomere (2007) presents a comprehensive review of all ship-generated wave components, further elaborating on nonlinear components, precursor solitons and their impact. The environmental impact of the range of ship waves is well documented and investigated for various marine species. Two review papers (Gabel et al., 2017; Byrnes and Dunn, 2020) elaborate on the main contributions of research on the general impact of shipping traffic on various environmental aspects. Gabel et al. (2017) present an overview of the different impacts ship-generated waves may have on different species. The authors stress the interrelation of different ecologically damaging aspects. Cascades of ecologic processes may be initialized that were often not fully understood at the time of publication. A newer review of the general impact of navigation on the environment has recently been published by Byrnes and Dunn (2020). The authors emphasize the variety of shipping related environmental concerns, comprising pollution, emission and physical disturbances, but only dedicate a small part of their work to the ship-generated wave systems. Du et al. (2020) provide an extensive literature review, focusing on ship hydrodynamics in confined waterways. The main aspects elaborated on are the increased resistance and the modification of the secondary wave systems, as ships enter confined waterways. The advances of computational modelling of ship hydrodynamics on the basis of Navier-Stokes equations independent of waterway characteristics are presented by Stern et al. (2013). The authors focus on high-fidelity tools detailing hydrodynamic processes in close proximity to the ship and the underlying numerical methods. For the effect of propeller or thruster jets causing scour due to ship maneuvering in harbours, the reader is referred to the respective review works (Lam et al., 2011; Wei et al., 2020).

This review paper differs from existing literature in that it specifically addresses long-period, primary waves and highlights its relevance compared to other ship-generated wave systems. Available information on loads induced on engineering structures, morphological processes of waterways, as well as specific flora and fauna are reviewed. These effects are inspected in parallel, as the governing causalities are related. Initially, the increasing size of sea-going ships and associated reports on intensifying ship-induced loads were the motivation for this literature review. However, the similarities of the hydrodynamic processes of ship-waterway interaction within inland waterways allow a certain transfer of knowledge to the coastal and estuarine context. At the same time, the authors are of the opinion that the derived conclusions can –to a large extent– be applied to inland waterways with complex bathymetries, as established within the framework of river restoration measures. Consequently, all types of confined waterways are within the focus of this review work. The specific objectives of this literature review are threefold: (i) to review the effects of primary waves on the waterway perimeter; (ii) to review methods for predicting characteristics of ship-generated primary waves and their effects; and (iii) to identify future challenges caused by commercial traffic on confined waterways.

The remainder of this review work is structured as follows. Section 2 firstly provides an introduction to the different wave systems of the ship wave field and presents earlier work looking into the impact of wave components other than primary waves. This section is intended to set a common framework and provide an understanding of the relevant processes on which then the relevant effects are analyzed. Subsequently, Section 3 focuses on the damage induced by primary waves, based on existing literature and new findings from the Elbe estuary. Methods commonly applied to determine primary ship waves are reviewed in Section 4. An outlook, discussing potential future challenges and the required research to address those, is given in Section 5. Finally the main conclusions are outlined in Section 6.

2 Components of ship wave systems

Different characteristic components of the ship wave field are reported in the literature. The relative magnitude of different ship wave systems are dependent on the ship size and speed, as well as the dimensions of the surrounding waterway. Long-period waves of remarkable magnitude are induced by large displacement ships progressing through confined waterways or smaller ships operating at high speeds in shallow water. Short-period secondary waves are generated by all types of ships. Each of the components may become critical from a design perspective, dependent on the naturally occurring loads at each site, the ship fleet navigating within the respective waterway, and traffic intensity. In the following, the ship wave systems will be introduced covering all wave components, thereby providing the necessary background information for Sections 3 – 5.

2.1 Primary wave system

A ship navigating through water causes variations in pressure and velocity of the surrounding fluid. As the ship progresses, the water volume displaced at the front is subsequently refilled towards the aft, causing a current alongside the ship, opposing the direction of the ships movement. The pressure is reduced alongside the ship, as the total energy remains constant due to Bernoulli's principle. At the free surface, this results in a lateral water level reduction. In contrast, stagnation points of the velocity field around a ship in motion at its bow and stern cause a local pressure increase and water level elevations at the respective points. From a stationary observer's perspective, the water level at the ship hull therefore exhibits a bow wave, a long trough alongside the ship, and a stern wave (see Figure 1) (Bhowmik et al., 1981; Oebius, 2000).

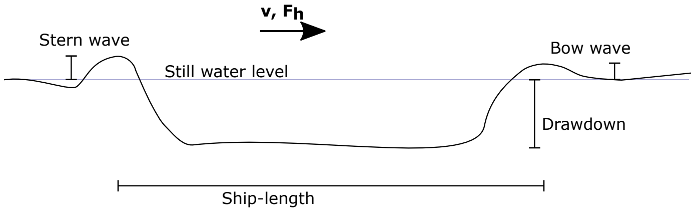

Figure 1: Sketch of the primary wave system parallel to the ship's main axis, where v denotes the ship's forward speed. The blue line indicates the still water level. The black line indicates the ship-induced free surface displacement (redrawn after CIRIA (2007)).

The above described lateral pressure reduction and the associated water level variations are qualitatively independent of the navigated waterway. However, lateral boundaries and a limited depth intensify the current velocity alongside the ship, due to the reduction of flow area (Bhowmik et al., 1981). This confinement effect causes higher magnitudes of water level depressions, such that the impact on the surroundings is only of interest in confined waterways (Bertram, 2002). According to Du et al. (2020), the confinement effect progressively increases depending on the ship and waterway dimensions: A lateral confinement starts to have an effect if the ratio of waterway to ship beam width is about 50-200, but only shows a significant impact when this relation exceeds a threshold of 10-15. Restricted depth exhibits an effect starting from a water depth of 15 times the ship draft and becomes increasingly important for a depth corresponding to 3-4 times the ship draft (Du et al., 2020). Even lower water depths starting at a draft to depth ratio of 1.5 - 2, are referred to as shallow water conditions. These are most intensely studied, as ship hydrodynamic parameters prove very sensitive within these waterways (Briggs, 2006; Briggs et al., 2010).

The water level variation caused by the flow field around the ship is called the primary wave system. Commonly, the term drawdown is used to describe the lateral water level depression in reference to the still water level (Taylor et al., 2007) (see Figure 1). The energy input from the bow and stern wave decays with distance to the ship, forming the secondary wave system (Bhowmik et al., 1981) (see Section 2.3). Due to the physical origins of the lateral water level reduction, the alternative terms depression wake (Scarpa et al., 2019), depression wave (Bellafiore et al., 2018), Bernoulli-wake (Rapaglia et al., 2011), wave-wash (Kucera-Hirzinger et al., 2009), wake-wash (Jiang et al., 2002), hull displacement waves (Ravens and Thomas, 2008), or drawdown wave (Taylor et al., 2007) are nowadays in use. Maynord (2004) and Houser (2011) use the term surge to describe the wave height measured from the initial depression to the stern wave. This component of the primary wave system is of particular interest as wave transformation processes, presented in Section 2.2, are reported to intensify the impact on the surroundings, as will be highlighted in Section 3. The current, opposing the ship's motion trajectory and refilling the displaced water volume, is termed return flow (BAW, 2010) or return current (CIRIA, 2007). In addition, a slope supply flow is following the ship, refilling the longside drawdown from astern (BAW, 2010). The currents induced by the primary wave system are depicted in Figure 2.

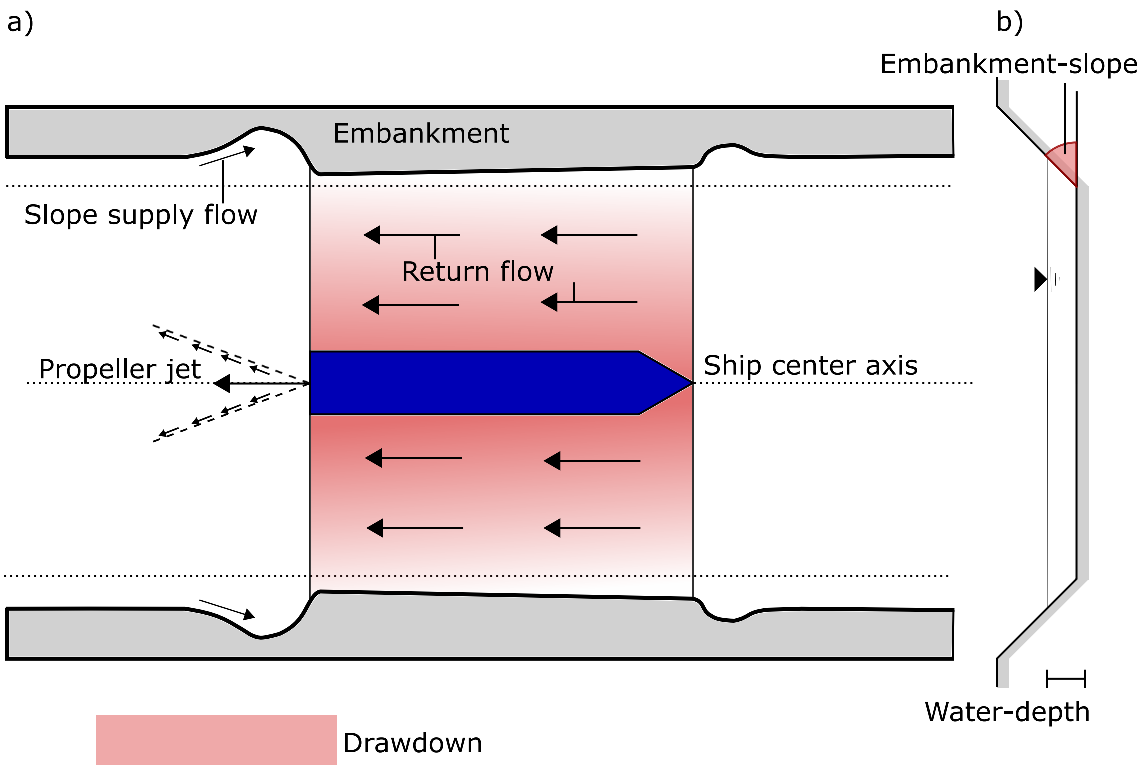

Figure 2: Schematic of the ship wave induced currents in a trapezoidal channel. a) top view and b) cross-section. The area highlighted in red indicates the drawdown (redrawn after Oebius (2000)).

The length of the drawdown wave corresponds to the length of the ship (Gharbi et al., 2010). Based on the physical nature of the wave and confirmed by field measurements (e.g. Bhowmik et al. (1981)), it is evident that the ship speed and the ship's cross-section in relation to the waterway cross-section are determining factors for the resulting wave heights. This has been taken into account in empirical equations, more thoroughly reviewed in Section 4. The water level drawdown and associated currents are critical, regarding erosion or biotic impact, as will be discussed in Section 3.

2.2 Deformation processes of the primary ship wave system

Ship-induced drawdown is assumed to decay with distance to the ship, resulting in largest magnitudes directly at the ship position while decreasing in distance to its source (Bhowmik et al., 1981; BAW, 2016). The distance in between the ship's sailing line and the gauge recording the progressing wave is, therefore, considered an important factor governing the impact on the waterway, which has been verified by field measurements by e.g. Matheja and Schweter (2007); Davis et al. (2009); Parnell et al. (2015). Since design-relevant primary ship waves are generated by large vessels, their wave-length is particularly long. Therefore the interaction with the waterway's bathymetry is significant as it is also governed by frictional losses and is equally affected by shallow water wave transformations. As a consequence, several authors report on deformation processes, including higher resulting wave heights in shallow water, as drawdown waves propagate away from the ship. The findings suggest a more complex relation of wave impact dependent on distance to the ship. The well-known shallow water wave transformations, shoaling, refraction and diffraction, and wave breaking are particularly relevant, and the complexity of the ship's wave dynamics is aggravated by non-uniform bathymetry.

The Venice lagoon has been extensively studied, as the mudflats surrounding the navigation channel used to access the port of Marghera, allow a pronounced development of deformation processes over a large distance. Field measurements in the lagoon revealed that ship-generated drawdown waves are symmetric on the boundaries of the navigation channel, but progressively deform during their propagation over the adjacent mudflats (Parnell et al., 2015). The authors report that the front slope of the drawdown wave becomes less steep during its propagation away from the ship, while the rear slope rapidly gains in steepness, eventually even exhibiting shock like features or breaking and formation of bore-type waves (e.g. see also (von Häfen et al., 2019)). These deformation process of the ship-induced wave are found to be accurately predicted by nonlinear theory, used to model the wave propagation (Parnell et al., 2015).

This is in agreement with the findings of Rapaglia et al. (2011), who observe the same characteristic shape for the propagating waves in the Venice lagoon. Flow velocities and associated sediment suspension is found to be largest in the vicinity of the rear slope, indicating the practical relevance of the deformation processes with regard to an accurate description of loads induced by primary waves.

Another study reporting on the characteristic deformation of ship-generated drawdown waves is given by de Jong et al. (2013). The authors describe the steep rear slope of the drawdown entering a shallow groin field, resulting in increased wave height and a partly breaking crest forming a bore. A video recording of the process allows a detailed analysis. Further field evidence of primary waves deforming into bore-type waves is recorded in a very shallow tidal Creek in Galveston Bay (Ravens and Thomas, 2008). These drawdown waves, generated in the adjacent waterway, were breaking, travelling upstream into the creek. In the bay, a drawdown could be measured prior to entering the creek; however, inside the creek no noticeable drawdown could be recorded, suggesting that the broken rear slope induced the sediment transport at the site.

2.3 Secondary wave system

The work addressing secondary ship waves, the visually most striking wave component in the overall ship wave field, was first observed and dates back to the end of the 19$^{\text{th}}$ century. Lord Kelvin was the first to document his studies of waves generated by a moving object in deep water (Thomson, 1887). The secondary wave system of a point source itself is composed of two types of waves, as depicted in Figure 3, namely a): (1) transversal waves move in the direction of the progressing source, (2) divergent waves move outwards away from the source. Both types of waves meet at the so called cusp-line. Its location in relation to the source can be described by a cusp locus angle (Thomson, 1887). In deep water, the cusp locus angle is independent of ship speed, forming the so called Kelvin angle with a constant magnitude of 19.47° (BAW, 2010). The significance of Kelvin's contributions is reflected within common alternative names for the ship's secondary wave systems, Kelvin wake (Soomere, 2007) or Kelvin wave system (Soomere, 2007).

The independently generated bow and stern wave systems (see Section 2.1) interact with each other during their progression within the waterway, adding to the complexity of the ship wave field of real ships (Du et al., 2020). In addition to that, other geometrical variations on the hull might cause independent wave systems but can generally be neglected for the ship geometries in operation (Bhowmik et al., 1981).

Kelvin's pioneering theory was extended to shallow water regions by Havelock (1908) as the author found that wave-bottom interactions affect the cusp locus angle, dependent on the ship speed and water depth. In his honor, the alternative name Havelock angle -for the cusp locus angle in shallow or intermediate water-depth- has been introduced in the research community. Havelock further introduced a valuable dimensionless number to describe ship wave related phenomena. The depth Froude-number F_h for shallow water indicates the ratio of the ship speed to the shallow water wave celerity $c = \sqrt{gh}$:

$$F_h = \frac{V}{c} = \frac{V}{\sqrt{gh}}, \tag{1}$$

where V is the ship speed, g is the gravitational acceleration, and h is the water depth. Ship speeds smaller than the wave celerity are referred to as subcritical ($F_h < 1$), whereas larger ship speeds ($F_h > 1$) are supercritical, and velocities of unity ($F_h = 1$) are considered critical. In realistic conditions however, such a clear distinction of the speed regime is not possible, resulting in a corridor of transcritical speeds in the range of $0.84 < F_h < 1.15$ (Soomere, 2007) (see Figure 3 b)).

Assuming linear wave theory, propagation in an inviscid fluid without surface tension, and a constant water depth allows the definition of a qualitative concept to describe the steady state wave pattern and an estimate of relevant magnitudes of the surface elevation (Soomere, 2007; David et al., 2017). Shallow water effects only become relevant starting from a wave length corresponding to twice the water depth. Considering characteristic lengths for both transverse and divergent waves, this results in a threshold for the transition from deep to shallow water conditions of about 0.55 to 0.7 for the depth Froude-number (Soomere, 2007). In shallow water, the Havelock angle continuously widens when passing this limit until reaching the critical speed. A maximal Havelock angle of 90° takes shape at a depth Froude-number of unity, e.g. $F_h = 1$, (Sorensen, 1997). In this case, both secondary wave components concord (Pethiyagoda et al., 2018). For supercritical ship speeds, the Havelock angle is decreasing with increasing Froude-numbers. The dependence of the Havelock angle on the relative ship speed according to Havelock (1908)'s theory is depicted in Figure 3 b).

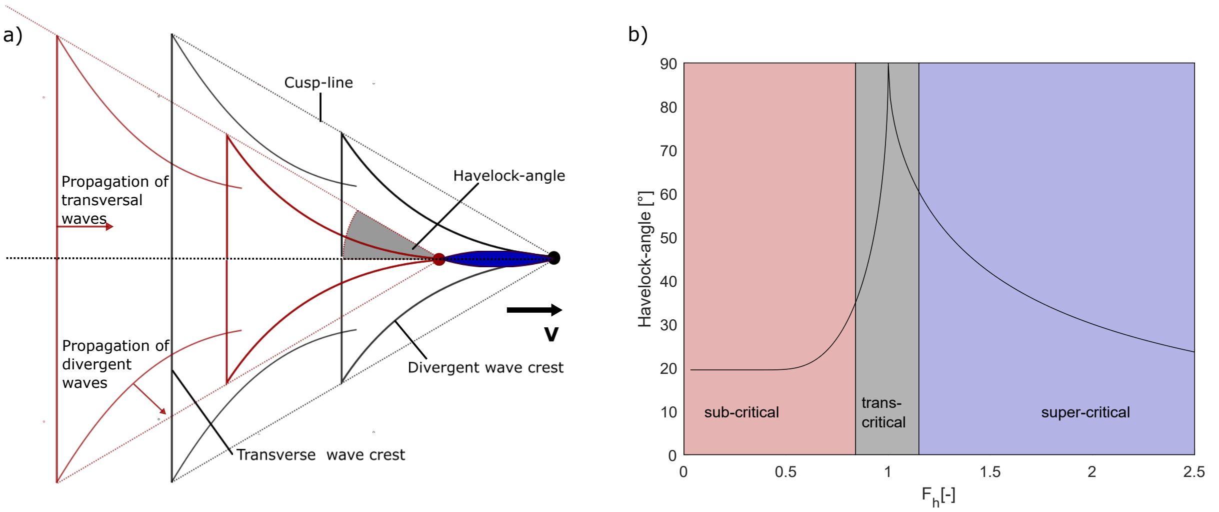

Figure 3: a) Secondary wave systems of a subcritical ship in shallow water (redrawn after Du et al. (2020)) b) Havelock angle dependent on the depth Froude-number (redrawn after Havelock (1908)).

The exact calculation of wave amplitudes and periods as they evolve through time and space, accounting also for nonlinear effects, requires sophisticated, often time-consuming analytical or numerical approaches (see e.g. (Lee and Lee, 2019; Pethiyagoda et al., 2018)). Some general characteristics of the relevant wave parameters of the secondary wave system can be introduced nonetheless. As the transverse wave crests widen up with increasing distance to the source, the wave amplitude is reduced. Highest waves can be expected along the cusp-line, since both secondary wave components superimpose each other there. The secondary wave periods depend on the ship speed. In deep water, the relation between wave period and ship speed is linearly proportional, by a factor of 0.52 (Soomere, 2007). In shallow water, the wave period is still increasing with increasing ship speed; however, no proportionality can be observed (Soomere, 2007).

Examples of studies looking into the damaging effect of ship-generated secondary waves focus either on relatively small ships travelling in sheltered waterways, characterized by absence of significant natural loads e.g (B. Bauer et al., 2002; Maynord, 2005; Parchure et al., 2007; Macfarlane et al., 2014; Bilkovic et al., 2019; Styles and Hartman, 2019; Shuster et al., 2020) or offshore structures where ships pass by closely (Dong et al., 2009). Reflections of secondary waves from the lateral boundaries are further known to complicate the wave field (Ji et al., 2012).

2.4 Solitonic precursor waves of ships operating near the critical regime

In addition to the drawdown and secondary waves described in Sections 2.1 and 2.3, precursor solitons can also become relevant. These periodically propagating components of the ship wave system originate from nonlinear wave components of the bow wave of ships navigating near the critical speed. Additional low energy components can develop within the cusp-lines as a result from nonlinear Bragg scattering of short and breaking waves, but their practical relevance is limited (Soomere, 2007). On the contrary, precursor solitons propagating ahead, generated by fast ships, are reported to induce characteristic loads in sheltered environments, inducing shoreline erosion (Kelpšaite et al., 2009).

The first description of a solitonic wave by Russell (1845), based on a ship progressing through a narrow channel pulled by horses, dates back to the beginning of the 19th century. Its generation can be explained by the balance of nonlinear and dispersive effects in the bow wave. Initially, the dispersive effect is small, so that the bow wave travels with the ship speed. Due to the ship's energy input, energy accumulates, leading to an increase in wave height. For a sufficiently large wave height, the dispersion results in a wave speed larger than the ship speed. The wave then starts to propagate away from the ship, conserving its mass, and therefore best being described by the solitary wave theory. After the detachment of the bow wave, this cycle starts over again, leading to a cyclic generation of such solitonic waves (Wu, 1987). For high ship speeds, breaking of the precursor soliton is documented, resulting in its propagation in form of a bore. A threshold for the depth Froude-number between 1.1 and 1.2 is identified as critical for breaking of solitonic precursor waves (Gourlay and Cook, 2004).

Even though well studied and described by analytical solutions (see e.g. Ertekin et al. (1986); Chen and Sharma (1995)), a growing interest for the quantification of solitonic precursors for design purposes emerged with an increasing number of high speed ships, such as fast ferries. Wave generation can be observed for ships operating at small velocities, but their magnitude only becomes decisive for ships operating near the critical speed (Soomere, 2007). Ship size in relation to the surrounding waterway is also governing the resulting wave height (Soomere, 2007). Transport ships, associated with relatively low speeds, are not reported to cause solitonic precursors. As an example, in the Venice lagoon, field measurements show that container ships operating in the region are not known to have generated any significant solitary waves (Parnell et al., 2015).

Due to their long period and the associated high energy fluxes, solitonic precursors are qualitatively different from naturally occurring wind waves (Soomere, 2005). A number of publications look in detail into the determination of solitonic ship waves and their effect on the waterway navigated e.g (Erm and Soomere, 2004; Torsvik and Soomere, 2008; Didenkulova et al., 2011; Wang and Cheng, 2021), and references therein. Primary waves and solitonic precursors are both characterized by their long period. However, their physical generation mechanisms are different and they arise under different operational and sailing conditions. Terms describing the wave components differ among previous publications. Some authors use the term *wake* to describe the entire ship wave systems (Soomere, 2007). Others use the term ship *wake* only for the secondary wave system, while precursor solitons and ship-generated drawdown waves are summarized under the term *wash* (Jiang et al., 2002; Garel et al., 2008).

2.5 Ship hydrodynamics in confined waters

The hydrodynamic processes induced when a ship progresses through a confined waterway do not only affect the surrounding waterway (e.g. bottom and embankments) but also change the loads acting on the ship, in turn affecting its maneuverability. Considering that the effects are originating from the same modification of the flow pattern within the medium surrounding the ship as the primary wave, advances from this line of research may inform further predictions of ship-induced loads. Therefore they are introduced in further detail.

Resulting from the water level depression, or rather the decrease in pressure alongside the ship, a vessel in motion is lowered in its position in relation to its position at rest at subcritical speed (Constantine, 1960). Comparable to the primary wave system, a ship in motion is always vertically displaced through the modified pressure distribution, but magnitudes only become relevant when lateral or depth confinement effects intensify the ship-induced currents (Millward, 1996). The reduction of underkeel clearance is called squat. It is composed of the contributors sinkage and the trim. Sinkage describes the vertical displacement of the entire ship, while trim refers to the angle setting in caused by an uneven change in position of bow and stern (Gourlay, 2011). Presumably, the magnitude of the squat equates to the drawdown directly adjacent to the ship (Bhowmik et al., 1981; Almström and Larson, 2020). The accurate prediction of squat is of great concern to waterways and estuarine traffic management, as otherwise serious incidents such as grounding might occur. For an overview of such past incidents see (Barrass and Derrett, 2013). In response to the trend of increasingly large ships entering sea ports, the question of an exact quantification of ship squat has recently become more urgent (Gourlay et al., 2015).

In case of critical or supercritical operation conditions, the ship is lifted above the still water level and a high constant trim angle is reached (Millward, 1996). To reach a supercritical condition the required power is high, so that usually only recreational boats, ferries, or small commercial ships operate in the supercritical regime.

Ships are designed with respect to their resistance when progressing through water, given that this largely affects the fuel consumption. Fuel costs contribute to 50 % – 60 % of the total shipping costs (Mallidis et al., 2018). In contrast to other costs, like crew wages and harbour fees, these costs are sensitive to ship design. Consequently, resistance has been intensively studied, aiming at optimal hull design but also resulting in a variety of observations connected to wave prediction. The resistance can be decomposed in the physical components viscous resistance and wavemaking resistance (Bertram, 2002). Various parameters contribute to the overall resistance, hull shape and speed being among the most prominent influences. Even though the share of each component on the overall resistance can not be measured directly, the separation into different types of resistance allows the development of conceptual descriptions of the components (Bertram, 2002; Dogrul et al., 2020).

Wavemaking resistance is of interest in both confined and deep water situations alike, since all wave components contribute to it. Wavemaking resistance itself can not be measured directly, resulting in experiments in towing tanks often used for an empirical quantification (Wilson et al., 1978; Moctar et al., 2012). Numerical models employed to predict wake making resistance commonly asses the quality of water surface prediction around the ship as part of model validation (Lv et al., 2013).

The viscous resistance encompasses resistance connected to local turbulence induced by the modification of the flow pattern surrounding the ship, as well as friction alongside the wetted portion of the ship hull due to the formation of a boundary layer. The accelerated flow due to the confinement effect as described in Section 2.1 induces additional friction alongside the hull (Linde et al., 2017). Therefore, the effect of a limited depth and the lateral confinement is highly relevant for the determination of the overall resistance with regard to the return current (Du et al., 2020). Barrass and Derrett (2013) quantify the effect of entering a confined waterway with a speed reduction of up to 75 % at constant power. The hull form of ships is of major importance to quantify ship-related parameters such as the combined resistance (Liu et al., 2011; Chi and Huang, 2016). In contrast, available literature indicates that far field properties of the ship-generated waves can be predicted by simple approximations of the hull shape (Macdonald, 2003; Almström et al., 2021).

The modified pressure and velocity field around a ship in motion causes an effect on other ships, either moored or in operation. Confinement effects are known to intensify the forces acting on other ships (Kriebel, 2007). Experimental studies comprising a towed ship passing by a moored one were performed by Kriebel (2007). The data set encompasses varying water depths, ship speeds, and passing distances in between the ships. It was confirmed that decreasing distance in between ships, increasingly shallow water, and increasing ship speed all contributed to significantly higher forces acting upon the moored ship. Maximal surge force (in direction of the ship centerline) and yaw moment occur when the passing ship's longitudinal center is at the position of the moored ship's bow and stern. The maximal sway force occur when the ships are alongside each other. At this position, the Bernoulli effect induces a force pulling the moored ship towards the passing one (Flory, 2002). Field measurements from the Elbe river, quantifying water level elevations resulting from ships passing a river parallel harbour, show the significance of these findings for practical applications (Matheja and Schweter, 2007). It is shown that large displacement ships induce highest wave components compared to smaller ships and, therefore, need to be considered critical for the mooring design. Further literature on the interaction forces of ships operating in confined waterways can for example be found in (Vantorre et al., 2002; Fenical et al., 2007; Zou and Larsson, 2013*b*; Flory and Fenical, 2014; Denehy et al., 2016; Pawar et al., 2019).

Figure 4: The drawdown is reproduced at a sloped embankment within an experimental test facility (Source: German Federal Waterways Engineering and Research Institute).

Figure 5: The secondary wave field of a container-ship deformed in vicinity to a sand bank due to shallow-water processes (Source: German Federal Waterways Engineering and Research Institute).

An additional force acting upon the ship can similarly arise when a ship passes nearby a lateral obstacle or navigates close to the waterway banks. The cause for this effect is analogous to the squat. The pressure in the area between the ship and the obstacle is decreased, due to an acceleration of the flow velocity. This pressure drop leads to a force sucking the ship's stern towards the bank (so-called bank effect), which can cause a moment turning the bow towards the waterway centerline (Lataire et al., 2009; Zou and Larsson, 2013*a*).

2.6 Section summary and highlighted concerns

The ship-generated wave field comprises the components of primary wave system, secondary wave systems and precursor solitons. The primary wave system, comprising a bow wave, a drawdown and a stern wave, magnifies in amplitude within confined waterways. The drawdown propagates away from the ship in the form of a drawdown wave as exemplified in Figure 4. Remarkable deformation of the drawdown wave, comprising a further increase in magnitude and wave breaking is reported within shallow water regions of the surrounding waterway. The dominant secondary wave systems, generated at the bow and stern of the ship, decay in form of short-period, oscillatory waves forming a multidirectional superposed wave field as depicted in Figure 5. They become most critical in waterways characterized by a load climate that is not affected by high-energy wind waves. Long-period precursor solitons are generated by fast moving ships in shallow water, operating at transcritical conditions, and are design-relevant in coastal waterways travelled by fast ferries. The aforementioned wave components comprised in the water level response to a sailing ship are the basis for an understanding of the effects that are observed along embankments of confined waterways. The next section will thus address impacts of those water motions on the associated effects on estuarine, riverine and coastal land-water interfaces.

3 Impact of ship-generated primary waves on confined waterways

The loads induced by water level elevations and currents generated by ship-induced primary waves are often anecdotally reported to be damaging to embankments. As a consequence, these hydraulic loads are potentially design-relevant in a large number of confined waterways frequented by large ships; these regions are mostly estuaries, canals, rivers, or coastal areas adapted to ship traffic by dredged channels. This review hence dedicates the next section to review the critical ship drawdown wave induced loads, as currently available in the permanent literature. Three main themes of damaging influences can be identified that will be presented in the following.

A large number of publications, introduced in Section 3.1, is looking into the morphodynamic activity induced by primary waves on specific sites. The second group, presented in Section 3.2, is concerned with damage to engineering structures, an issue not studied intensively to date. As an additional novel contribution in this work, some findings of previous research on damaging influence of primary ship waves on embankments are displayed; these are often only available as technical reports and supplement the summary knowledge collected in here.

The direct environmental impact on various species living within the waterways is studied by several authors and collated in Section 3.3. The potential impact of erosion and turbidity on environmental conditions is clearly evident (e.g. Kucera-Hirzinger et al., 2009), but as the implications also concern other questions like bank design as well, they are introduced separately. In addition, one source was found where a deformed primary wave has proved fatal for a person (de Jong et al., 2013).

Due to the relatively large number of publications, the main methods and findings are summarized in form of tables for the respective category in the associated section. Additional remarks are then given afterwards, highlighting, for instance, magnitudes of the quantities determined. Throughout this section, the category "ship fleet" refers to the relevant ships considered in the respective publication a priori or identified as relevant within the conducted research. However, ships travelling a waterway are not necessarily restricted to this type of vessel. Further, the information provided on ship types largely differs among the publications, resulting in a mixed specification dependent on purpose and exact parameters.

3.1 Sediment suspension caused by ship waves

Table 1 shows the research that studied the effect of primary ship waves on morphological dynamics of waterways. The reviewed publications comprise erosion processes, as well as increased turbidity induced by an increased concentration of suspended particles as depicted by means of example in Figure 6.

For the estuarine environment of the Hillsborough Bay, FL, USA, Schoellhamer (1996) quantifies the effect of primary waves in relation to naturally occurring wind waves. The author reports that the yearly mass of sediment re-suspended due to primary ship waves is an order of magnitude higher compared to the mass shifted by wind-generated waves.

A field study on the Savannah River, GA, USA, reveals that supercritical pilot boats and subcritical container ships can both contribute to sediment re-suspension. Both types of ships have a characteristic wave pattern: the drawdown is significant for the container ships travelling by, whereas pilot boats generate shorter waves. The direction of the sediment transport induced by container ships is usually landwards, whereas pilot boats induce an offshore sediment transport. At that study site, both types of ships are in operation simultaneously, so their wave systems superimpose, requiring a combined analysis on effects induced by both types of vessels (Houser, 2011). Measurements of three-dimensional (3D) flow velocities and suspended sediment on the Danube river considering the activity of medium sized cruise ships highlight the impact of primary ship waves compared to secondary waves (Fleit and Baranya, 2021). The time series of the measured quantities is analytically decomposed into the components induced by primary and secondary waves. Even though primary wave velocities are usually smaller compared to the secondary components, the associated unidirectional velocity leads to a large erosion potential, while the oscillating water column of the secondary waves results in an almost zero cumulative sum of transported sediment. Due to the complexity of the processes involved, the authors suggest the combined use of field measurements and different numerical tools in the far and near field for future analysis.

In the Venice Lagoon, extensive field measurements correlating ship data from the Automatic Identification System (AIS) with turbidity sensors, velocity metres, and pressure sensors reveal a strong impact of the shipping intensity on the sediment suspension in the lagoon mud flats (Scarpa et al., 2019). The lagoon is navigated by large ships entering the port of Marghera through a dredged channel, connecting to the Adriatic Sea. The ship-induced drawdown waves in combination with the surrounding low-lying marshes can lead to significant nonlinear deformation. The supposedly moderate drawdown alongside the ships is reported to magnify its amplitude when it propagates into the shallow flats resulting in a drawdown wave of up to 2.45 m. A pronounced vertical velocity component is measured to cause an increase of suspended particle concentration from about 30 mg/L to more than 500 mg/L. The authors of that study stress that the findings can be projected onto other locations as similar navigation situations occur globally. In the same region, remote sensing, the employment of historical maps and bathymetric surveys indicate a correlation of shoreline regression and ship traffic, with an annual shoreline retreat of up to 4 m/year (Zaggia et al., 2017). It is concluded that drawdown waves are the main reason for erosion, due to the low frequency of storm events compared to ship passages. Gelinas et al. (2013) specifically attribute the increase of sediment concentration in the Venice Lagoon to the primary wave of a passing ship. Due to the low water level in the surroundings, the drawdown covers a large part of the water column, leading to flow velocities exceeding 2 ms^{-1} in maximal cases. The resulting turbidity measured

Table 1: Constraints and main findings of the publications looking into erosion induced by primary waves

Author(s)	Location	Method	Waterway	Ship fleet	Damaging Component	Impact
Plate and Keil (1971)	Kiel Canal, Germany	Field data, Experiments	Channel	13,000 Gross register tons	Return current	Bank erosion
Ulm et al. (2020)	Kiel Canal, Germany	Field data	Channel	Increasing in size due to lock adaption	Return current	Ship-induced sediment transport
Schoellhamer (1996)	Hillsborough Bay, FL, USA	Field data	Estuary, dredged channel	Large ships (L= 100 m to 250 m , D = 7 m to 13 m)	Drawdown wave	Sediment resuspension
Dauphin (2000)	St. Lawrence waterway, Canada, USA	Field data	River	Commercial traffic	[-]	Bank erosion
Gaskin et al. (2003)	St. Lawrence waterway, Canada, USA	Experimental data	River	[-]	Complete ship wave system	Bank erosion
Garel et al. (2008)	Wootton Creek, UK	Field data	Estuary, dredged channel	Car ferries (L = 77 m,B=17 m, D = 2.5 m)	Horizontal velocity	Shoreline erosion
Ravens and Thomas (2008)	Houston ship channel, TX, USA	Field data	Tidal creek, adjacent to channel	[-]	Bore-like deformation of drawdown rear slope	Sediment transport into creek
Davis et al. (2009)	Aransas Wildlife Refuge, TX, USA	Field data	Tidal creeks, adjacent to estuary	Barge trains	Creek velocity increased by drawdown	Increased bed load sediment flux
Houser (2011)	Savannah River, GA, USA	Field data	River mouth	Container ships, pilot boats	Horizontal flow components	SSC-increase
Schroevers et al. (2011)	Scheldt-estuary, Antwerp, Belgium	Field data	Tidal flats adjacent, to dredged channel	Container ships	Ship wave induced currents	Erosion suspected
Gelinas et al. (2013)	Venice lagoon, Italy	Field data	Dredged channel	Container ships, cruise ships	Velocity of progressing wave	Increased turbidity, erosion
Zaggia et al. (2017)	Venice lagoon, Italy	Field data, remote sensing	Dredged channel	Container ships, cruise ships	Progressing drawdown wave assumed from previous literature	Shoreline retreat
Scarpa et al. (2019)	Venice lagoon, Italy	Field data, results from previous measurements	Dredged channel	Container ships, cruise ships	Vertical and horizontal velocity component of progressing wave	Channel and shoreline erosion
Göransson et al. (2014)	Göta Älv, Sweden	Field data, empirical equations	River	L =85 m,B = 15 m ,D = 5 m	Correlation to Drawdown	Increased turbidity
Larson et al. (2017)	Göta Älv, Sweden	Field data, empirical equations	River	L =85 m,B = 15 m ,D = 5 m	Correlation to Drawdown	Increased turbidity
Duró et al. (2020)	Meuse, Netherlands	Field data	River	Class 3-ships	Currents at shallow areas due to drawdown	Erosion at renaturalized banks
Mao and Chen (2020)	Grand Canal, China	Field data	Inland canal	Barges, Yachts	Correlation to drawdown	Sediment resuspension
Fleit and Baranya (2021)	Danube, Hungary	Field data	River	River cruise ships	Primary wave induced offshore currents	SSC-increase

SSC: Suspended Sediment Concentration

along with maximal velocities corresponds to a re-mobilized sediment layer of a couple of millimeters thick after the passage of a single ship. Recently, the unusually clear water in the Venice Lagoon during the start of the SARS-CoV-2 pandemic, and the associated lockdown, found its way into public media (e.g. CNN (2020)). The analysis of satellite imagery reveals the impact of the reduced shipping traffic on the turbidity within the lagoon, alongside with low precipitation and positive seasonal effects (Braga et al., 2020).

Schroevers et al. (2011) present measurements from the Scheldt estuary, navigated to access the port of Antwerp, comprising quantifications of water level and current velocity at two locations 30 m and 230 m away from the navigation channel. The results qualitatively agree to the ones from the Venice Lagoon, even though the gauge density is not as high there. Primary waves reach a significant height of up to 0.7 m on-site and propagate far over the surrounding flats, exhibiting larger wave heights at the gauge further inshore, presumably a result of wave deformation processes. As a consequence, shear stresses are higher at the distant gauge, with values of $2.5\,\mathrm{N\,m^{-1}}$. Secondary wave heights are larger; however, they reduce quickly when travelling away from their origin given the shorter duration and lower momentum. An impact on the region's morphology is suspected, but not further quantified.

Relatively small drawdown magnitudes are already found to have a significant impact on the erosion of unprotected banks. At the Wootton Creek, UK, field measurements of turbidity, velocity, and pressure indicate a significant impact of the drawdown on sediment re-suspension compared to the ship's secondary wave system (Garel et al., 2008). Even for a moderate drawdown of 0.13 m, an increase in the Suspended Sediment Concentration (SSC) from about 25 mg/L previous to the ship passage to 150 mg/L after its passage is recorded. Sediment analysis suggests that displaced material originates from upper beach levels. The authors conclude that low gradient beaches are subject to erosion as the long-period primary wave can travel to areas of a beach usually above the high water line.

Sedimentation occurring at tidal creeks adjacent to intensively travelled waterways shows to be highly sensitive to local conditions and constraints, particularly with respect to the effect of primary waves. Davis et al. (2009) present field data indicating an increase in the offshore sediment transport, driven by the water level fluctuations at the river outlet induced by ship drawdown. Ship-generated drawdown waves were found to have a moderate magnitude of about 0.1 m but still range in the order of the tidal variations. Bed load sediment flux doubled in connection to a drawdown wave approaching the mouth of the creek. Ravens and Thomas (2008) report on upstream sediment transport into a tidal creek, induced by primary waves generated in the adjacent waterway. A plug of sediment is described that completely blocked the creek, with possible severe consequences for the drainage of the adjacent areas. It was found that primary waves break at the location, forming a bore transporting sediment up into the creek. A bore height of up to 0.11 m was measured in a location of only 0.13 m water depth. The opposing sediment transport direction on both sites, depending on bathymetry, primary wave height and tidal creek discharge, highlight the need for detailed site-specific assessment of primary wave impact.

3.2 Damage to engineering structures

Navigated waterways can be protected from erosion by constructing riprap along the banks, by using dykes to prevent damage of the surroundings resulting from flooding events, or by installing groins and training walls along the waterway to ensure safe operation conditions. Ship-generated primary waves exert loads on these structures, and waterway agencies and governmental bodies aim to stabilize or protect embankments within their administrative boundaries; most often, due to the lack of adequate guidance for primary wave loading, these design works are guided by designers' experience and expert knowledge. There is a number of publications, among them publicly available technical reports of case studies, reporting on observed damage and looking into the examination of the impact on these types of structures. An overview of the different studies is given in Table 2.

Table 2: Constraints and main findings of the publications looking into engineering structures damaged by primary waves

Author(s)	Location	Method	Waterway	Ship fleet	Damaging Component	Impact
Taylor et al. (2007)	Burlington shipping channel, Canada	Field data, numerical model	Channel	Seaway-max, L = 225.5 m, B=23.7 m, D=8.1 m	Return current	Scour around sheet pile walls
Kunz (1977)	Elbe estuary	Field data	Dredged channel	[-]	Water level variations by drawdown	Quickly accelerated tidal gates
Uliczka et al. (2009)	Elbe and Weser estuary	Field data	Dredged channel	Large container ships	Water level variations drawdown	Quickly accelerated tidal gates
Ohle and Zimmermann (2003)	Elbe estuary	Field data, numerical model, experiments	Dredged channel	[-]	Currents induced by primary waves, in conjunction with wind waves	Rocks of riprap embankment displaced
BAW (2018)	Elbe and Weser estuary	Experiments, numerical model	Dredged channel	Large container ships	Drawdown induced waterlevel differences in groin fields	Displaced rocks on groins and training walls
Melling et al. (2019)	Elbe estuary	Field data, experiments	Dredged channel	Large container ships	Drawdown induced waterlevel differences in groin fields	Displaced rocks on groins
Melling et al. (2020)	Elbe estuary	Previous research, monitoring	Dredged channel	Detailed analysis, L=100 m to 400 m	Drawdown induced waterlevel differences in groin fields	Displaced rocks on groins

Significant scour has been observed at the piers and entrances constructed using sheet pile walls of the Burlington shipping channel, connecting Lake Ontario to Hamilton harbour. Field measurements indicate that near bed velocities, occurring during the passage of large ships, reach a value of up to $1.6\,\mathrm{m\,s^{-1}}$, a value that exceeds the ones recorded at a hurricane event (Taylor et al., 2007). Equally, a study by Lojek et al. (2021) indicates an influence of vessel operation on the sedimentation pattern around the berthing of the Dagebüll harbor, Germany, that is hypothesized to be substantially influenced by the normal ferry service that is connecting to the island of Föhr. The berthing in the Dagebüll harbor has a foundation consisting of closely-spaced piles on which a slab is resting, and the tidal and ship-induced flow dynamics are specifically difficult to untangle in the geometrically complex harbor setting.

In Germany, the seaports of Bremen and Hamburg are located on estuaries, causing these waterways to be travelled intensively and leading to high ship wave induced loads. Several unpublished reports and publications look into damages induced on training structures alongside these estuarine waterways. In the region, storm surge protection measures are in use, aggravating the complexity of the combined tidal, estuarine and ship operation impacts. Small drainage channels are connected to the estuary by means of sluice gates ensuring the draining of the typically low-lying hinterland when tidal water levels drop to levels where free surface outflows develop. These gates operate automatically depending on the hydraulic pressure at either side of the gates. Kunz (1977) was the first to report on rapid movement of such gates caused by primary ship waves. The rather sudden pressure changes induced by ship-induced primary waves, compared to natural periods of events like storm surges, lead to high acceleration and "slamming" of the gates, exceeding the design loads. Further measurements on Elbe and Weser estuaries, including wave gauge data and gate motions, emphasize the importance of considering ship-induced loads during gate design (Uliczka et al., 2009). The authors report the gates to be highly sensitive to ship parameters, speed among the most relevant factors.

Displacement of the riprap protecting the embankment was observed along the Elbe estuary, leading to further investigations on the driving factors and mechanisms causing damage (Ohle and Zimmermann, 2003). A framework of methods, comprising field measurements of water level data throughout an entire year, numerical modelling, experimental studies, and analytical concepts of loads and failure, led the authors to the conclusion that a combination of wind waves and ship-generated waves are a plausible cause for the failure. The highest measured drawdown reached a magnitude of 1.53 m. The riprap was not designed to withstand this additional loads, resulting in partial or sometimes entire embankment failure.

In German estuaries, river training structures in form of rock groins extending into the waterway and training walls parallel to the navigation route are used to ensure safe navigation and prevent erosion of the banks. Over the past two decades, increased damage and displacement of rocks forming these structures has been observed, initialising further research into damage mechanisms associated with primary wave structure interaction. Field measurements at the Langlütjen training wall in the Weser estuary revealed water level differences of 0.6 m either side of the wall during ship passages (BAW, 2018). Erosion of the slope facing the navigation route was observed, caused by high velocity overflow processes of the training wall in response to the water level gradient.

Significant damage to a number of groins in the Elbe and Weser estuaries are also attributed to primary wave induced loads. The interaction of the drawdown and stern wave with the rock groins typically results in a very characteristic damage pattern, where the groin root - the transition region between the groin and the adjacent bank - and the lee-side of the groin body are severely damaged. The damage mechanism includes a focussing of wave energy in the groins' root area and high-velocity turbulent overflow of the groin in response to a water level gradient originating from the drawdown (Melling et al., 2020). The erosion tendency as a result of ship traffic is thought to be moderated by the influence of the ambient tidal water level which influences the exposure of the groin to overflow loads, though further scientific insight is still scarce. Based on an understanding of these processes, optimised groin designs were designed on the basis of the observed damage pattern and tested in 3D physical model tests (BAW, 2018). In addition, the new designs were also examined in a prototype study, testing two different groin designs in the Elbe estuary where the incident primary wave loads and damage development of the groins were monitored over several years (Melling et al., 2020). Despite improvements to the structural stability achieved by modification of groin geometry, the importance of validated design methods for rock sizing in response to overflow loads is noted (Melling et al., 2019).

3.3 Environmental impacts

Several mechanisms specific to primary waves are reported in the literature to be detrimental to flora and fauna living near the embankments of waterways (see Table 3). The ecological concerns attributed to these interactions has become an increasingly important aspect in operation, maintenance, and planning of waterways. Adams et al. (1999) show how a water level reduction on sloped banks at rates corresponding to ship-induced drawdown can cause young fish, typically living near the banks of Mississipi river, to remain on the dry part of the slope (strand) following the passage of the ship. This effect is associated with typical behaviour of different fish species, either opposing a current or drifting with it. The highest stranding rate observed for one species left 66 % of individuals on the dry slope. Similarly, the return currents induced by ships are reported to exceed the swimming capacities of young fish, putting them under additional stress or causing displacement from their natural habitat (Wolter and Arlinghaus, 2003; Wolter et al., 2004; Kucera-Hirzinger et al., 2009).

Table 3: Constraints and main findings of the publications looking into direct impact of primary waves on species

Author(s)	Location	Method	Waterway	Ship fleet	Damaging Component	Impact
Ali et al. (1999)	Nile, Egypt	Field data	River	River cruise ships	Unspecific, only correlation	Plants displaced
Adams et al. (1999)	Mississipi, MO, USA	Experiments	River	[-]	Drawdown	Fish stranding on slopes
Wolter and Arlinghaus (2003)	[-]	Literature	River	Commercial ships	Return current	Fish washed out
Wolter et al. (2004)	Oder-Havel-Kanal, Germany	Field data + Analytical model return velocities	Inland channel	Commercial tows	Return current	Fish washed out + stressed
Kucera-Hirzinger et al. (2009)	Danube, Austria	Field data	River	Varied	Return current + velocities from other components	Fish stressed, increased turbidity
Pearson and Skalski (2011)	Columbia River, OR, USA	Field data	River	Deep-draft vessels	Drawdown	Fish stranded
Schludermann et al. (2014)	Danube, Austria	Field data	River	River cruise ship, Cargo ship	Drawdown	Reduction of larval densities
Liedermann et al. (2014)	Danube, Austria	Field data	River	River cruise ship, Cargo ship	Drawdown	Habitat retreat
Silinski et al. (2015)	[]	Experiments	Intertidal Marsh	unspecific	Long waves, used to model primary waves	Drag forces on plants

Plants develop specific survival strategies dependent on their habitat. Silinski et al. (2015) compare the survival strategies of the pioneering plant species *Scirpus maritimus* turning mudflats into vegetated marshes. Full scale experiments show that stress tolerance at different vegetation phases is sufficient to withstand the short-period wave induced loads resulting from wind waves, typically occurring in the plant's habitat. Long-period waves, used to model drawdown waves, exceed the plants resistance against drag forces and cause plant tissue failure. This indicates that the species' survival and, therefore, the development of a stable marsh vegetation in general is endangered by ship-generated primary waves.

Liedermann et al. (2014) perform measurements on the Danube river to identify critical wave components generated by different ships acting upon river banks. The authors conclude that primary waves generated by large and slow ships, such as bulk carriers and passenger ships, are most relevant for inducing stress on the banks. Largest drawdowns of 0.4 m are observed on the study site. These drawdown magnitudes caused a significant waterline retreat (of up to 35 m), on gently sloped banks, resulting in temporal habitat loss for aquatic animals. Accompanying monitoring of larval densities on the site further highlights the determining impact of primary ship waves at these shallow sites, especially valuable as nursery habitats for fish (Schludermann et al., 2014).

In addition, a primary wave has also been reported to cause a human fatality, a potential danger well known in coastal communities as exemplified in Figure 7. On the Nieuwe waterway, an approach channel to the port of Rotterdam, two anglers were swept off their feet on 25th April 2011 and pulled into the water, by a wave generated by a passing PANAMAX container ship (de Jong et al., 2013). The shallow foreshore of the location, established via a groin field, contributed to the steepening of the surge component of the wave, which could be regarded as critical in this case.

3.4 Section summary and highlighted concerns

A primary conclusion of the existing literature on ship-generated waves is the large variety of the effects of shipping activities on the built and living environment, depending on each specific site and the local traffic patterns. The height of drawdown waves can become remarkable, like in the Venice Lagoon, but even drawdown waves of smaller height may cause severe problems, as shown by Garel et al. (2008). Different processes associated with primary waves are reported to be critical, encompassing return flow, currents induced by the progressing drawdown wave, and associated water level variations. A unifying factor among all reviewed publications,

Figure 6: Shipping traffic can have a determining impact on a waterway's sediment transport as depicted here for the Kiel Canal (Source: German Federal Waterways Engineering and Research Institute).

Figure 7: The threat of ship-generated waves and currents is well known in coastal communities; however, it has received relatively little attention in scientific literature (Source: German Federal Waterways Engineering and Research Institute).

including the ones focusing on ecological concerns, is the relevance of bathymetric influences. This is reflected within the governing impact of waterway dimension upon the magnitude of the drawdown wave. However, equally important is the bottom interaction during wave propagation leading to wave deformation. The impact of drawdown waves on banks and beaches of rivers and coastal waterways alike is intensified in the case of relatively flat and shallow swept areas. Compared to other processes relevant for the design of engineering structures and morphological stability, such as wind waves, secondary ship waves, and river discharge, primary waves can become the critical load case, greatly exceeding naturally occurring loads. Their long period distinguish primary waves from oscillating waves, like wind waves or secondary ship waves, forming a qualitatively new load. The specific load parameters of drawdown waves regularly lead to failure of biological survival strategies and established construction guidelines alike. The reviewed literature exhibits an increasing demand to better understand, to simulate and predict the effects, and eventually plan for the primary waves as induced by ship traffic in complex bathymetries. To that end, the next section is providing a review of and limits to the existing prediction methods of ship waves; this knowledge and the conclusions drawn will then lastly allow for the identification of future research needs with respect to ship-generated waves.

4 Established methods to predict ship-generated waves

The impact of ship-generated primary waves can be considerable, as highlighted in Section 3. Therefore, the design of structures and the assessment of the morphological and ecological consequences arising from planned modifications of waterways or a change in the shipping fleet, requires tools for predicting the associated hydrodynamic processes. Field measurements are indispensable to enhance process understanding within existing waterways. However, they provide insufficient when it comes to predicting future loads.

Experimental, analytical and empirical methods can be useful to predict such loads. Yet, the generation and propagation of ship-generated primary waves is highly site-specific, limiting the applicability of these methods. Experimental methods are time-consuming and expensive, as the replication of the bathymetry of the waterway is required. Analytical methods require several simplifications, in order to be able to find solutions. Empirical methods rely on regression-functions to in-situ and experimental data. Such methods all have in common that reliable results can only be obtained in relatively simple waterway geometries, like inland channels. The wide range of parameters and the number of variables affecting the propagating drawdown waves in coastal waterways and near-natural rivers results in inaccurate prediction of loads in complex bathymetries. Numerical methods can overcome the issues mentioned. Nevertheless further developments are required, to obtain reliable results at reasonable computational costs.

To that end, the following section is dedicated to review methods to predict ship-induced primary wave action acting on the surroundings, focusing on the advances in numerical modelling of ship waves. The abilities of contemporary tools are highlighted and further research needs are shown. Even though experimental, analytical and empirical methods have their limitations in predicting wave loads in spatially variable waterways, they prove valuable for analysing conceptual relations or hydrodynamic details of the examined waterway and their drawbacks can be moderated by combining them with numerical methods. Therefore this section starts by briefly reviewing them as well.

4.1 Experimental, analytical and empirical methods

Experimental models allow studies with a more controlled parameter space, compared to field studies. As propagating primary waves are largely dependent on local bathymetry, experiments are time consuming and expensive. Experimental test campaigns to assess the impact of ship-induced loads on bed erosion, banks, tidal gauges, and other ships were performed prior to modifying the Elbe (Uliczka and Walte, 1996) and Weser (Uliczka and Kondziella, 2006) estuaries by dredging. The experimental set-up comprised towing tests of ships passing through a scaled section of the respective river, including bathymetric features like groins and and adjacent tidal creeks. The method provides detailed insights in the propagation of waves within the specific river section. However, a choice needs to be made, which part of the river becomes subject to the more detailed analysis, on basis of either experience or field data collection. The large amount of parameters affecting primary wave generation and propagation complicates the adequate choice of the critical section and limit the validity of the obtained data for the entire river. Recently, the adaptation of groins was also informed by experimental modelling (BAW, 2018). Besides further towing tank experiments, a detailed analysis of processes occurring during stationary and wave overtopping of scaled groins was included. This requires a large numbers of tests to be performed, due to the number of parameters considered in the design phase of groins. The characteristic parameters of ship-generated primary waves can to date not completely be reproduced in conceptual models replacing the moving ship by other wave generation mechanisms. Hence, the assumed loads only partly account for the hydrodynamic processes taking place during a full scale ship passage.

Scaled model tests in towing tanks for different geometries and different hull shapes deliver important data for determining ship squat and resistance; they are commonly used as validation data for numerical tools. Examples are given by (Lataire et al., 2012; Ciortan et al., 2012; Elsherbiny et al., 2019; Du et al., 2020). A commonly used reference case is the publicly available Duisburg Testcase (DTC), representing a 14,000 TEU Post-PANAMAX hull, developed only for validation and benchmarking purposes (Moctar et al., 2012). A common issue often discussed amongst experimental researchers is the effect scale has on the accuracy and reliability of the results. Scaling theory is governed by relevant force similarity, while other forces are intentionally neglected. For ship towing tests , meaningful experimental campaigns commonly require the similitude of both Reynolds and Froude numbers (Bertram, 2002). A review of the different scaling approaches for depicting ship-hydrodynamics has been recently conducted by Terziev et al. (2022). Despite a careful design of the experimental test, scale effects, resulting from additional forces not covered by the scaling approach, affect the results. The induced errors can be partly mitigated by empirically-based extrapolation procedures. Yet, the remaining inaccuracies along with tedious experimental procedures are often a reason to employ other methods or to combine different methodological approaches (e.g. towing tests with CFD simulations).

Analytical frameworks for the determination of ship-waterway interaction were originally developed to quantify the ship squat. Later, the developed slender-ship approximation was also applied to determine ship wave properties. This approach is still commonly used in numerical tools to inform flow properties at the ship's location, some of which are introduced in Sections 4.2.1 and 4.2.3.1. An analytical approach to quantify the squat phenomenon in shallow water was developed by Tuck (1965), later extended to laterally confined waterways (Tuck, 1967) and to only partially confined, dredged, channels (Beck et al., 1975). The thin-ship method of Michell (1898) assumes the beam to be small, compared to the ship's length. The slender-ship approximation used by Tuck (1965) additionally assumes the relation of draft to length to be small. Based on the potential flow theory and an asymptotic expansion, an analytical solution is found. The hydrodynamic pressure, the vertical force, and the trim moment are obtained. Sinkage and trim can be calculated for the hydrostatic case, based on the determined forces. A comprehensive overview of Tuck's contributions and subsequent work is given by Gourlay (2008, 2011). Blaauw and van der Knaap (1983) summarize the early advances of analytical squat prediction.

For many years, empirical equations, derived from experiments or field measurements, have been the dominating method to generalize the results and to predict drawdown induced currents and squat. Present design guidelines for bank and bottom protection of inland waterways mainly rely on empirical equations (BAW, 2010; CIRIA, 2007). The assumptions required for applying the existing guidelines include constant rectangular or trapezoidal cross-sections, water-depths, and ship speeds. These assumptions are applicable to artificial inland channels and to some extent to navigated rivers. A new equation for the diameter of armour protection units of riprap at river embankments is presented by Kurdistani et al. (2019), including more input parameters than previously considered within the guidelines. The authors found their equation to be applicable within a large parameter space, but still constant ship speed and bank slope need to be assumed to apply the suggested equation.

In addition to the equations included within guidelines, various other equations were suggested to determine drawdown and squat, each predicting the respective underlying data sets with high accuracy. A list of these equations, specifically designed to address drawdown, is compiled in Table 4, including the respective parameters used for determination. Further information on the data sets used to derive the equations are described by Almström and Larson (2020).

Table 4: Collection of publications postulating empirical equations for drawdown prediction and the required input parameters

Author(s)	V	r	A_S	A_C	g	L	d	D	T	h	C_B
Schijf (1949)	•	•	•	•	•						
Gelencser (1977)	•		•	•		•	•				
Dand and White (1978)	•		•	•	•						
Bhowmik et al. (1981)	•		•	•	•	•	•				
Hochstein (1967)	•	•	•	•	•						
Maynord (1996)	•	•	•	•	•		•		•		
Kriebel and Seelig (2002)	•				•	•				•	•
CIRIA (2007)	•	•	•	•	•				•		

V: Ship speed
r: hydraulic mean-depth
A_S: Ship cross-section
A_C: Waterway cross-section
g: Gravitational acceleration
L: Ship length
d: Distance ship-shoreline
D: Ship draft
T: Waterway top
h: Water-depth
C_B: Ship-block coefficient

The cross-sectional areas of ship A_S and waterway A_c are commonly put into relation forming the channel blockage factor S

$$S = \frac{A_S}{A_C}. \tag{2}$$

The simulation of a ship progressing through a uniform waterway using Computational fluid dynamics (CFD) for various dimensions of waterway widths and depths (see also Section 4.2.2) suggests that a coefficient like the blockage coefficient is not sufficient to predict resistance in a confined waterway (Linde et al., 2017). The authors conclude that separate values for width and depth restrictions need to be included. Melling et al. (2020) suggest the use of a partial blockage factor, which includes the cross-sectional areas of ship and waterway on each side of the midship section, thereby emphasizing the effect of a decentral sailing line of the ship and a potentially asymmetric waterway cross-section. Field data from the Elbe estuary reveals a strong dependence of the measured wave height to the partial blockage coefficient.

Comprehensive introductions to the variety of empirical equations for squat prediction are given by Briggs (2006) and Briggs et al. (2010). All of the empirical formulations for drawdown and squat are limited to predict maximal respective height and neglect the wave period, which is important for predicting the loads induced by the propagating drawdown. Particularly for morphodynamic studies and effects on embankments the effective duration, which is closely coupled to the wave period, is an important parameter controlling the displaced sediment volumes.

Almström and Larson (2020) present data from a field campaign in the Stockholm Archipelago and compared it to the complete set of equations for predicting drawdown and the additional equations for squat prediction given within this section. Large ships like passenger ferries and cruise ships are identified to be the most relevant sources for primary waves in the area of interest. Their data upon passage is retrieved from AIS information and combined with continuous water level measurements at two points. The comparison of the established empirical equations shows that the prediction is rather poor, yielding maximal coefficients of determination of 0.48. The relatively poor agreement is explained by the dependence of the local wave characteristics on the bathymetry. This coincides with findings from Göransson et al. (2014); Larson et al. (2017), who compared the prediction quality of drawdown height in the Göta River with the drawdown formula of Kriebel and Seelig (2002) and a squat formula. Based on the presented references, empirical equations can hence be considered to be of insufficient accuracy for the design of engineering structures based on detailed load analysis, due to the importance of local bathymetry for wave generation and propagation and the wide parameter space controlled by the respective shipping fleet. To that end, Almström and Larson (2020) present a novel empirical approach by introducing a site-specific regression formula, based on the relatively simple field data collection with a stationary installed water level gauge. The obtained results yield better agreement with field-data compared to the previously used equations.

A different approach for processing field data is presented by Luo et al. (2022). The authors present a machine learning technique to identify ship waves from a data set of a navigation channel in a shallow estuary region and distinguish it from wind waves. The high recognition rate of ship wakes (93.55 %) indicates the good performance of the approach. Machine learning techniques such as the presented one contribute to an efficient analysis of large data sets and can therefore help to ultimately develop future prediction methods.

In addition to water level elevations, currents induced by the displacement effect of ships can become relevant during the design process. Methods to predict return flow velocities are suggested in CIRIA (2007); BAW (2010). However, the absolute magnitude of the velocity is only one of several parameters governing the loads on the embankments. Further determination of local velocities as a function of the (local) bathymetry is required, as the ship-induced velocity field is spatially diverse (Maynord, 1996; BAW, 2010). In addition, empirical equations predicting slope supply flow are presented in BAW (2010). This flow component may become relevant for breaking stern waves of ships travelling close to the banks.

4.2 Numerical Methods

A variety of numerical methods have been developed to predict the interaction of a ship with the surrounding confined waterway. Methods based on potential flow theory (see Section 4.2.1) or CFD methods, based on Reynolds-averaged Navier-Stokes equations (RANSE) (see Section 4.2.2), are more commonly applied for the quantification of ship centric attributes, such as squat and resistance. Methods to predict the phenomena are ship centric, usually neglecting the important deformation processes governing wave parameters in the far field. However, established methods in this field of study enable the prediction of far field waves or can be adapted to determine the relevant processes on the far field scale as well. Therefore, most common methods for squat and resistance prediction are also reviewed in this section. Depth-averaged methods, presented in Section 4.2.3, are to date more common to predict ship-induced loads on the waterway.

As introduced in Section 2.5, studies to predict squat and resistance commonly assess the wave field surrounding the ship for quality evaluation of the numerical tools and to quantify wavemaking resistance. In naval hydrodynamics, many additional questions are of interest, such as seakeeping (the motion response of a ship to wind waves), the propeller effect, or processes in the air phase around the ship. These additional questions, and the commonly used methods to answer them, are beyond the scope of this review. However, the interested reader is referred to (Stern et al., 2013) for an overview of the progress in ship hydrodynamic methods over the past 30 years.

4.2.1 Potential Flow

Potential flow theory requires several assumptions on the flow field in order to be valid and applicable to in-situ settings. The flow is assumed to be incompressible, inviscid, and irrotational, ultimately reducing the equations for the mass and momentum conservation to the Laplace equation. Turbulent energy dissipation is neglected. The Reynolds number resulting from typical ship dimensions and speeds is large in non-confined water, resulting in limited influence of viscous processes and the evolution of thin boundary layers. Hence, potential flow theory has found wide application in naval hydrodynamics in deep water conditions. Boundary-element-method (BEM) solvers, providing solutions in frequency domain, are most commonly applied to solve the Laplace Equation in the field of wavemaking resistance prediction (Bertram, 2002).

In the following, a brief overview of the BEM, used for wavemaking prediction, is given following the standard text book of Bertram (2002). First, the surface of the fluid is discretized using a number of panels, reducing the dimension to a 2D problem (Zhang et al., 2020). A set of boundary conditions is introduced, including a no-penetration condition at the water surface, the ship hull, and any additional boundaries representing waterway restrictions. In addition, the Bernoulli-equation is imposed at the free surface in its nonlinear or linear form. Lateral boundaries and the sea floor in the shallow water case can be included as symmetry planes or as impermeable surfaces. Mirror images of the same strength as the original sources can represent symmetry planes when positioned in symmetry to the original sources. This results in zero normal velocities at the boundaries. Rankine sources are commonly applied as boundary integral equation, first suggested by Dawson (1977). The solution procedure is repeated until a steady state solution is found. Examples of the Rankine-panel method (not specifically for confined waterways) are found in Shahjada Tarafder and Suzuki (2008); Härting et al. (2009); Lv et al. (2013); He and Kashiwagi (2014); Peng et al. (2014); Mucha and Moctar (2014); Chen et al. (2016).

Alternatively to the Rankine sources, Green-Functions can be employed. Examples relying on the Green function in the boundary integral equation are presented by Huang et al. (2013); Abbasnia and Soares (2019). A simpler boundary condition, making use of the analytical work of Tuck (1967) introduced in Section 4.1 and relying on the slender body approximation, is presented by Gourlay (2014) and further elaborated by Terziev et al. (2018) for the tool *ShallowFlow*. In this code, the ship is included as a line of sources, imposing limitations to the representation of the actual ship hull.

Models relying on potential flow theory cannot be used to predict viscous resistance in confined waterways, due to the theory inherent assumptions. However, several researchers suggest methods to predict sinkage and trim in confined waterways relying on potential flow assumptions. Results concerning sinkage are emphasized here, regarding the close connection of sinkage and primary waves. Yao and Zou (2010) present a BEM-based method to predict ship squat in confined waterways on the basis of Rankine Sources and an image method for the waterway bottom. Numerical convergence could only be obtained for ships moving outside the critical regime. Results are compared to an experimental data set of moderate confinement ($S = 0.032$) (Jiang, 1998), showing only minimal deviations of predicted sinkage in the subcritical regime. A similar BEM relying on Rankine sources is presented by McTaggart (2018). Two experimental data-sets are used for validation of confined conditions. The increase of sinkage with increasing ship speed under subcritical conditions is predicted. For very moderate confinement ($S = 0.032$), as studied by Jiang (1998), results are excellent. In case of more intense confinement (S=0.13-0.18) , magnitudes differ by approximately 60 % compared to the reference data of Lataire et al. (2012). Sinkage is qualitatively underpredicted by the model under all operation conditions. Gourlay et al. (2015) compared two potential flow theory methods to several experimental data sets of container ships: *GLRankine*, a BEM based on Rankine sources, and *ShallowFlow*. The experimental data comprises different modern container ship hulls progressing in shallow water, aiming at squat and trim prediction. Even for moderately confined cases, predicted midship sinkage differs up to 50% compared to the reference. For cases of more intense confinement, *ShallowFlow* underpredicts sinkage throughout the entire range of Froude-numbers. The Rankine source method is only applied to one case of moderate confinement, indicating better results. Still, deviations of about 25 % can be observed.

Alderf et al. (2011) introduce a field method based on potential flow theory. The numerical solution method is based on the finite elements method, accounting for unsteady squat as a function of the local bathymetry. The reference frame is ship fixed, while the bathymetry moves relative to the ship. The effect of underwater dunes, leading to a periodic variation of water depth and an abrupt underwater step, resulting in a sudden decrease in water depth, are examined. Stable solutions were obtained for ship speeds up to a depth Froude-number of $F_h = 1$. Varying squat in relation to depth variations could be predicted qualitatively, but due to a lack of corresponding experimental reference data, no quantitative validation could be performed.

4.2.2 RANS-CFD

The incompressible Navier-Stokes equations describe the physical processes within a waterbody, including all relevant nonlinearities, such as viscous effects (Zhang et al., 2020). High spatial and temporaral resolution is required, as turbulent processes take place on a small scale (Ferziger and Perić, 2002). The publications reviewed in the field of naval architecture rely on Reynolds-averaged parametrization of turbulent dissipation. Numerical methods using the Reynolds-averaged Navier-Stokes equations are more efficient than direct numerical simulations as the required resolution of the spatial and temporal discretization is reduced. The conservation of mass still requires a relatively high resolution, despite the recent advances in developing conservative discretization schemes for the free surface determination (Hong et al., 2005; Vukčević et al., 2016). If no sufficiently high resolution is chosen, numerical diffusion occurs, resulting in wave height reduction during their propagation. Thus, the possible range of applications is limited to relatively small domains and short simulation time periods.

In the last decade, CFD codes became increasingly popular to predict hydrodynamics of a ship progressing through a narrow waterway. Applications focus on steady state parameters of a ship progressing at uniform speed. Domain dimensions and simulated time can remain moderate for steady cases, rendering RANSE computations feasible. Resistance and squat are most intensively studied. Water level elevation data directly on the ship hull is regularly included in order to asses the reliability of the calculations (Lv et al., 2013). Other parameters than squat and resistance can be quantified as well, since RANSE solvers simulate actual hydrodynamic processes in the entire domain with high precision. Such additional quantities include, for instance, waves propagating away from their origin. Solutions are obtained in time domain, making it possible to simulate a ship progressing through a variable bathymetry at variable speed. However, the required computational resources are too demanding for applying them on real bathymetries and large domains like estuary regions or natural rivers using contemporary hardware (Rodrigues et al., 2018; Bellafiore et al., 2018).

The simulations of Bechthold and Kastens (2020) are a representative example of the required resources for a squat prediction simulation and illustrate the problems associated with questions requiring larger domains, such as ships progressing through large varying bathymetries. The authors simulated ships progressing steadily within a domain of 4.5 times the ship length for 400 s. Only then a steady state of the ship's position was reached. Simulations for this case took several days on 32 to 96 cores, according to the authors. Modelling a real coastal bathymetry, where significant primary waves propagating into the surroundings could be observed (see Section 3), would presumably require domains several orders of magnitude larger. Expected computation times resulting from such a simulation renders such an approach unfeasible for determining loads induced by various ship types. In addition, the numerical diffusion, potentially critical for CFD approaches when modelling wave propagation over long distances, may further reduce the applicability to large domains.

Examples of the application of RANS CFD tools in open waters can be found in e.g. Ciortan et al. (2012); Dogrul et al. (2020). Lately, promising results could be obtained by RANS CFD codes to predict hydrodynamics of ships in confined waterways, many of them employing commercial codes. As an example, validation studies concerning the use of CFD to predict ship hydrodynamics in confined waterways are discussed in the following.

Ji et al. (2012) study the confinement effect in a scaled waterway with sloped banks using the CFD code *ANSYS-Fluent* and compare their results to experimental data. In comparison to other publications, three wave gauges on the waterways banks at a distance of 1.2 m, 1.8 m, and 2.2 m from the ship's sailing line are included. The predicted drawdown on the foot of the bank deviates from the experimentally determined data by 10.7 %. The model is later extended by including the effect of the propeller and determining the sediment re-suspension induced by a ship in a narrow channel (Ji et al., 2014). Suspended sediment transport is modelled using a 3D-model that correlates fluid velocity and Suspended particulate matter (SPM). Linde et al. (2017) also used *ANSYS-Fluent* to assess the prediction of resistance and drawdown and compare numerical results to results from empirical models and experiments. One finding is the importance of updating the vertical ship position of the advancing ship in the model and, therefore, to include sinkage, in order to reliably predict the resistance in the numerical model. In contrast to empirical equations, the resistance predictions from the numerical simulations are within the range of uncertainty of the experimental data, given with $5 - 8\,\%$ for resistance and $1 - 2\,\%$ for sinkage, even for cases of highly confined waterways. Maximal deviations for sinkage are larger, yielding differences of approximately 30 %.

Tezdogan et al. (2016) use the solver *Star-CCM+* to model the behaviour of the DTC-hull operating in an asymmetric waterway at various draft and speed conditions. The results for squat prediction fall within the range of uncertainty in the corresponding experimental data. A case study to predict ship behaviour when navigating a conceptual model of the Suez Canal is presented by Elsherbiny et al. (2020). Numerical results from

Star-CCM+ are compared to experiments and empirical equations. The experimental measurements of the ship squat and the CFD results show good agreement for a generic (rectangular) and a more realistic (trapezoidal) channel configuration. In contrast, the results from the slender-ship approximation differ from the CFD solution. Depth Froude-numbers and associated sinkage magnitudes at the Suez Canal are low, due to speed restrictions. Maximum measured sinkage is 3.2 mm. The authors emphasize the uncertainty of measuring sinkage below 2 mm in experiments. Terziev et al. (2018) model the DTC-Testcase for several waterway configurations, including a deeper trench in the middle, surrounded by shallow areas. This represents a typical real-world configurations of dredged channels as analytically already studied by Beck et al. (1975). Qualitative agreement of the results is shown, using empirical equations and Beck's slender body theory, because of the absence of comparable experimental data. The effect of variations in the bathymetry on resistance and the wave field opened by the ship is included in a numerical study by Terziev et al. (2020), based on *Star-CCM+*. The modelled case comprises a progressing ship passing over a forward facing step in the bathymetry. The simulations show a significant increase in primary wave height when passing the step, alongside with an increase in resistance. Bechthold and Kastens (2019) and Bechthold and Kastens (2020) further validate *Star-CCM+* and illustrate its robustness by comparing the numerical results to 69 experimental configurations, including the DTC-Testcase. Blockage coefficients range from 0.029 to 0.1 and ship speeds range from 0.57 m s^{-1} to 1.3 m s^{-1}. It was found that squat is predicted with deviations of less than 20 % corresponding to an absolute value of 0.33 m in prototype scale. These deviations for extremely shallow cases are attributed to the omission of the propeller influence. A special form of channel is studied by Huang et al. (2021). The authors examine an ice channel, generated after deploying an ice-breaker that additionally cleans the channel from the remaining floes. Different from built channels, the open-water ice channel is only restricted at its surface while no confinement occurs underneath the ice surface. The results of CFD simulations with *Star-CCM+* indicate secondary wave reflections within the channel and an increase in resistance depending on channel width and ice-thickness. To date, the literature on ice-channels, especially concerning primary waves, is limited. However, the emerging intensification of navigation activities in the arctic oceans indicate a rising interest in studying this type of ship-waterway interaction.

Results of the CFD model *ISIS-CFD* for the steady solution of a ship advancing in a waterway is introduced by Lungu (2020). No validation data is provided, but the results are in qualitative agreement with observations in the reference data. The water surface along the ship is included, showing a strong dependence of the draft to depth ratio for the calculation of the drawdown.

Du et al. (2020) show the effect of the confinement of a navigated waterway. The authors perform simulations in the open source code *OpenFOAM* for two different shipping convoys, typically navigating in inland waterways, and compare the numerical results to experimental data. A lateral drawdown along the hull is shown, increasing with increasing ship draught and decreasing waterway width. The ship squat is neglected to simplify the analysis, but secondary waves and resistance match well with the experimental reference, with an maximum error of 8 % for the entire range of considered depth Froude-numbers.

The potential flow theory and RANSE-CFD both find wide application in the field of naval architecture. Dependent on the required accuracy and the expectations of turbulent dissipation affecting the flow field, a suitable approach should be chosen. With the increased availability of computational resources, more demanding numerical approaches, based on the RANS equations, have recently gained popularity for the analysis of confined operation conditions and deep water alike. Nonetheless the efficiency of potential flow theory based tools still renders them valuable for early design stages and routine tasks (Noblesse et al., 2013). Several researchers show that inviscid models can predict wavemaking resistance with sufficient accuracy for deep water conditions (Ma et al., 2018) or within a rectangular waterway neglecting squat and trim (Abbasnia and Soares, 2019). Kim et al. (2011) compare results from RANS CFD to an in-house BEM solver for the prediction of the wave pattern around a ship progressing in non-confined conditions. The compared information encompasses pressure on the hull and the water level at several longitudinal and transverse cross-sections. Employing experimental reference data, the results show that CFD is more accurate in the vicinity of the ship, while far field waves are more accurately predicted by the potential flow based method. The authors assume that numerical diffusion, smoothing out gradients, is the cause of the inaccuracies of RANSE-CFD for far field predictions.

For confined waterways, the literature comparing the quality of potential flow based tools compared to RANS-CFD is limited. Mucha and Moctar (2014) and Mucha et al. (2016) compare results from models based on BEM to solutions from commercial RANSE-based CFD solvers. The studies investigate a container ship progressing through a confined waterway of varying depth. All methods, including the ones based on slender-body approximation (Tuck, 1967), predict sinkage and resistance qualitatively well for low depth Froude-numbers. The deviations between viscous, inviscid, and experimental results become more evident for increasing confinement and higher ship speeds, where the RANS method yield more accurate results for sinkage in both studies. The interested reader is referred to the original manuscripts for a graphically representation of the results from the comparative study. Maximal deviations of squat prediction, determined visually, are about 10 % for the RANSE methods, about 15 % for Rankine-Source method, and about 30 % for the slender-ship approximation for a draft to depth-relation $d/h = 1.3$. Further comparison of RANS-CFD and potential flow results is presented by Zou and Larsson (2013*a*), highlighting the more accurate results from viscous methods.

The discussed results highlight the advantages of RANSE for the analysis at higher confinement and Froude-numbers. Higher confinement results in close proximity of viscous layers forming at the ship and the waterway bottom, and therefore turbulent processes are of major importance (Zeng et al., 2020). In this case, processes within the real fluid deviate from the ones assumed when applying potential flow theory. It can be concluded that potential flow theory based tools are suitable to efficiently predict steady state parameters of ships progressing in deep water or moderately confined waterways. Increasing confinement results in a rise of viscous effects, leading to less accurate results in these cases. Viscous methods based on RANSE predict ship squat more accurately in confined waterways. In addition, viscous resistance of ships can only be predicted by high-fidelity tools, therefore achieving a more complete quantification of ship hydrodynamics. An additional drawback of many suggested potential flow methods is that BEM solvers seek results in the frequency domain. This makes BEM unsuitable for predicting far field waves of ships progressing through varying bathymetries, due to the unsteady nature of the involved processes.

Finally, regarding the modelling of the interaction between ship-induced waves and river banks, Fleit et al. (2016, 2019) employ the finite difference based RANSE tool REEF3D::CFD (Wang et al., 2020*a*). The authors focus on the determination of hydrodynamic loads acting on river banks, necessary for the quantification of the environmental impact of ship traffic on species living or breeding on the banks. The studies rely on experimental input of the water elevation caused by passing ships to provide adequate boundary conditions for a reliable analysis. The littoral zone is reproduced in a numerical wave tank, representing a 2D-slice model of the sloped bank. The measured wave spectra are used as boundary condition for the generation of irregular wave trains in the CFD model. With this input given, shoaling and wave-breaking along the river bank are modelled. The spectral information at the stations on the slope shows a qualitative good agreement between CFD and measured data, even though the maximal amount of total kinetic energy is overestimated by the numerical model. The authors conclude that CFD computations prove to be a reliable tool in reproducing the ship-induced wave run-up on the embankments.

4.2.3 Depth-averaged numerical methods

The reduction of the dimensions of a domain greatly accelerates the computational solution procedures and, therefore, allows the calculation of larger domains and longer simulation times. Several numerical models are presented that are based on depth-averaged equations, either in form of the Boussinesq equations or the Shallow-water-equations (SWE), for predicting loads induced by waves propagating away from the ship generating them.

4.2.3.1 Boussinesq equations

The underlying concept of the Boussinesq equations is in the following described in accordance with a text of Madsen and Schäfer (1999). The vertical information is conserved by replacing the depth coordinate by a polynomial approximation describing the vertical flow field. The application of the equations is limited by nonlinearity, describing the relation of amplitude to water depth, h, and their dispersion, characterized by the relation of wave amplitude to wave length, L. While it was initially required that both quantities were small, some effort has been dedicated to overcome these limitations. Adapted equations were developed that allow the application in a wide range of water depths while maintaining dispersion characteristics and taking into account nonlinear effects. Consequently, these equations allowed to predict transformation processes of wind waves, such as shoaling and refraction. Commonly, the limits of applicability of the specific approximation is given in terms of kh, where k is the wave number $k = \frac{2\pi}{L}$. Madsen and Schäfer (1999) report on a number of $kh = 6$ as a threshold for the application of the Boussinesq equations. The numerical treatment of the equations is challenging, due to the inclusion of higher order derivatives and mixed time space derivatives (Jeschke et al., 2017).

Jiang et al. (2002) employ a slender-ship approximation in the near field, while making use of a Boussinesq type model for the propagation of waves in the far field, as proposed by Chen and Sharma (1995) in use of the

Kadomtsev-Petviashvili-equations. The slender-ship approximation results in local values for the velocity and the water level, used as boundary condition along the ship center line. These values depend on ship dimensions and the blockage coefficient. Results are computed and compared to an experimental data set for a fast ferry operating at supercritical and subcritical conditions in three different waterways. The waterways comprise a trapezoidal one, a rectangular one, and one corresponding to a dredged navigation channel. The domain length is large, including 17.5 times the ship length. Results are increasingly well predicted with growing distance from the navigation line.

Dam et al. (2008) use the same approach and compare the predicted results with field data sets from ships sailing in a confined river. Water level data from wave gauges positioned above sloped banks in relatively shallow water are used for comparison. The ships passing by are relatively small (Length: 26 m and 24 m). As a result, the wave field is dominated by secondary waves, instead of primary ones. The maximal secondary wave heights are predicted reasonably by the model, but the time series of water level elevation differs significantly.

An alternative approach for representing a moving ship in a Boussinesq type model is presented by Torsvik et al. (2009). The authors use a pressure disturbance imposed at the free surface of the Boussinesq model *COULWAVE* (Liu and Wu, 2004) to study waves generated by a transcritical ship progressing through a dredged channel. The wave amplitude is sensitive to the waterway geometry and ship speed, but no detailed assessment of the validity of the approach is performed. Ersan and Beji (2013) present a detailed comparison of results obtained from a Boussinesq model, based on Beji and Nadaoka (1996), with analytical results. Two different pressure terms are used for ship wave generation. One is a simple hemisphere, the other one corresponds to the shape of a slender body. Results are compared with regard to the prediction of the Havelock angle, which yields good results with an average deviation of 6 % for subcritical Froude-numbers.

Another model making use of a pressure term for predicting ship waves is presented by David et al. (2017). The *Boussinesq Ocean and Surf Zone (BOSZ)* model by Roeber and Cheung (2012) is extended by a pressure term representing a moving ship. The model is able to reproduce the speed dependent Havelock angle correctly. Furthermore, its practical relevance is showcased, comparing the numerical results to data obtained from a ship navigating through the port of Hamburg. The results are in good agreement, but since the ship is small, no significant primary wave is included in the time series.

Similarly, Rodrigues et al. (2018) show results for the adapted Boussinesq type code *FUNWAVE* of Nascimento et al. (2009), making use of the pressure term and comparing the results to data from experimental measurements, comprising wave gauges at various distances from the sailing line in a rectangular channel. The ship operates in a velocity range between $0.8 < Fr < 1.2$. The results show that the decay of the maximum wave height along the gauges is predicted accurately. El Safty and Marsooli (2020) employ the *FUNWAVE* code to study erosion in a shallow salt marsh region in Jamaica Bay, NY, USA, showing the practical applicability of the approach. Field measurements of wave spectra are performed for model evaluation. AIS data later indicates that the generated wave trains originate from a tugboat. Its dimensions are therefore used as input in the subsequent numerical simulations. The simulations reveal the importance of the frequency of the ships passages for erosion; however, due to the dimensions of the ship, primary waves were not in the focus of the assessment. Forlini et al. (2021) address the problem of different time scales included in the determination of the impact of ship waves on a waterway. The authors suggest to combine numerical simulations with statistical approaches, allowing to identify the long-term effects of the wave climate. Numerical simulations are used to determine characteristic wave patterns of various ship-types, yielding the input to subsequent multivariate stochastic analysis. In the study it is verified that *FUNWAVE* covers a sufficiently large range of parameters. Results indicate that there are limitations for small and slow ships, due to the restrictions of Boussinesq-models to replicate the dispersion characteristics. However, the ship wakes, determining the morphological activity including the drawdown, are accurately depicted by the numerical model.

A different method to include a moving ship in a Boussinesq type model with the aim to predict far field waves is presented by Morioka et al. (2020). The method consists of superposed Gaussian pulses representing the various wave frequency components resulting from the surface disturbance by the ship. The optimal configuration of each component is determined by an initial calibration data set, consisting of wave gauge data in reaction to a passing ship. Compared to results from experiments, the model shows good prediction accuracy and robustness for wave characteristics. Primary waves are not included, but the authors suggest the use of an own set of Green's functions within the Gaussian pulse for future inclusion in the model. A post-Boussinesq model presented by Samaras and Karambas (2021), making use of the slender-body pressure approximation by Ersan and Beji (2013), can predict the analytical Havelock angle correctly. Further, the numerical results agree with an additional experimental data set from a towing tank. Results of a ship entering a harbor basin show qualitatively plausible results including the reflections from harbour breakwaters.

The presented studies on Boussinesq type models show promising results in representing ship waves by the relatively simple numerical extension of an additional pressure field. However, the literature is limited to relatively small ships often sailing in the transcritical regime. Recent data (Forlini et al., 2021) indicates a good performance of Boussinesq models for the range of parameters of large sea-going ships. Yet, further validation with data from field and towing tanks experiments is required to examine if the shallow-water deformation processes are also replicated.

4.2.3.2 Shallow-water-equations (SWE)

Similarly to the Boussinesq theory based tools, the SWE also provide the possibility to study the effect of ship waves on a larger scale, while being efficient and taking into account the influence of the bathymetry. The underlying assumption is that the vertical length scale is small compared to the horizontal one. This assumption holds for primary ship waves, considering the large relative primary wave length (Gharbi et al., 2010). The wave length dependent dispersion relation is not necessarily included in the equations, in contrast to the Boussinesq equations. This may become problematic when considering rapidly varying bathymetries or waves of small length (Jeschke et al., 2017). Including a non-hydrostatic pressure gradient in the vertical profile allows to capture the dispersion relation numerically (Jeschke et al., 2017). This simpler assumption make the SWE more suitable for advanced numerical implementations, such as high order discretization schemes compared to Boussinesq equations (Wang et al., 2020*b*). In the literature, several examples are given where models based on SWE are successfully applied and are shown to reproduce measured time series dominated by primary waves well.

Stockstill and Berger (2001) present a hydrostatic shallow water model aiming towards the prediction of drawdown induced currents in off channel regions. The ship is included via a surface pressure term moving through the domain. Validation shows a very good match at various measurement locations of the Mississippi river. This model is later denoted *HIVEL2D* (Maynord, 2004). The additional validation for *HIVEL2D* presented by Maynord (2004), comparing numerical results to field data, shows very good agreement with field data from the Sabine Neches Waterway for a deep draft ship. Deviations of the water level are less then 20 %. The time series used for validation exhibits a pronounced deformation in form of a steep rear slope of the drawdown wave as presented in Section 2.2. This is well predicted by the numerical model. Further data showcasing the capabilities of the model is presented by Maynord (2003). Hammack et al. (2008) present a modified version of the methods of *HIVEL2D*, based on the same assumptions but computationally more efficient, introducing mesh adaptation abilities. Comparison to field data shows a good prediction for wave gauges positioned within a complex bathymetry along the Mississippi river.

Another model making use of a moving pressure field boundary and the SWE named *SGH* (Ship-generated hydrodynamics) is presented by Macdonald (2003). The wave field is decomposed in secondary and primary components, each computed separately from each other. Wetting and drying of cells due to the variations in water level is accounted for by a dynamic adaptation of the boundary conditions. Compared to field data from a tanker passage in the Corpus Christi Channel an excellent match for the drawdown prediction is presented for a realistic hull shape. Results are presented merely graphically, but virtually no difference between predicted and measured magnitude of 0.55 m is observed. Gharbi et al. (2010) present extended validation data for the tool *SGH* with a field data set collected in the St. Lawrence waterway. The data show favourable agreement for the passage of two different container ships with a respective length of 245 m and 295 m at two different wave gauge locations. The initial drawdown is predicted satisfactorily in period and height for most ships and gauges. However, an over-prediction of drawdown height of up to 50 % can be seen at one gauge.

Ship-generated waves can be included via a local increase in the term describing the atmospheric pressure (de Jong et al., 2013) within the open source model Xbeach. The software solves the nonlinear shallow-water-equation, either under hydrostatic pressure assumption or under non-hydrostatic, then requiring several vertical layers. The accuracy in capturing the structural shape of the hull depends on the resolution of the computational grid. Results are compared to validation data from an experiment of a ship passing an underwater slope adjacent to an extremely shallow water area (Lataire et al., 2009). Three wave gauges are included along the slope. A comparison with the reference data set shows that the code is capable of predicting primary wave characteristics precisely. Steepening of the drawdown rear slope is observed in the experiments and predicted by the numerical model. A more detailed validation was performed by Almström et al. (2021) on basis of field data from the

Stockholm Archipelago. Within the complex bathymetry of this waterway a good agreement of the measured and numerically determined primary-wave height and period could be obtained, characterized by a mean absolute error of 3 cm and 6 s, respectively.

Delft3D is another model relying on the shallow-water-equation that can be used to study primary ship waves (Lesser et al., 2004). Here, the ship is again included via a pressure term corresponding to the local draft of the ship (Zhou et al., 2013). Comparison with the experimental data set of Lataire et al. (2009) shows that the water level is well captured, regarding the primary wave system. Within the qualitatively presented results, no significant deviations between the experimental and numerical results can be observed. The model is highly sensitive to the choice of the horizontal eddy viscosity, necessitating the choice of a high value, almost completely dampening the secondary waves.

Parnell et al. (2015) and Rodin et al. (2015) model the primary wave propagating over the flats at Venice lagoon using the fully nonlinear SWE in one dimension. The aim is to predict the deformation observed at the site, as mentioned in Section 2.2. The initial drawdown was induced by a negative Gaussian pulse, determined on the basis of a field data set. Comparison to field data suggests that the approach describes the introduced deformation processes qualitatively well. The model does not account for wetting and drying of cells, resulting in poor prediction when these phenomena are observed in the field data-set. Bellafiore et al. (2018) equally use a SWE tool to model wave propagation of the primary wave over the flats in the same region. The initial water level drawdown is calculated by a CFD code solving the RANSE in the nearfield of the ship. The CFD code is coupled to a SWE tool, further predicting the wave deformation. The field data set used for validation comprises various water level gauges on a 1650 m long transect orthogonal to the sailing line. The water level time series adjacent to the channel, as well as wave attenuation taking place during the propagation over the flats, are predicted within the confidence interval at most gauge locations.

5 Future tasks

5.1 Future challenges

5.1.1 Developments in the shipping fleet

Despite the ever growing dimensions of sea-going container ships in the past, it can not be assumed that this trend can be extrapolated into the future. The main driver of the increasing ship capacity was a reduction of cost per container (Cullinane and Khanna, 1999). Building costs, as well as the relative crew cost and operation cost for powering and maintenance, on a per container basis were decreasing with enlarged ships. On the other hand, the required infrastructure at ports, technical constraints in ship building, and external risks like natural hazards accumulating within single ships limit the economical benefit of ever increasing ship sizes (Lian et al., 2019). The combined risks of mega ship operation and the vulnerability of international trade, dependent on bottleneck waterways, lately became evident when the Suez Canal was blocked by a wedged container ship (BBC, 2021). Still, the number of input variables affecting the optimal ship size render a prediction of future ship sizes difficult (Cullinane and Khanna, 1999).

More than twenty years ago an optimal size of 8000 TEU was predicted by Cullinane and Khanna (1999), a threshold greatly exceeded nowadays. A more recent publication predicts an optimal size of 18,000 to 20,000 TEU, if port costs are considered in the assumptions (Lian et al., 2019). This value is already exceeded by present day largest ships (Marine Insight, 2021). Experience from the past development of ship dimensions suggests that a further increase in transport capacity would rather result in larger ship beams, than further increase in draft or length (Garrido et al., 2020). Park and Suh (2019) stress the need for adapting port infrastructure if the past growth of container ships is extrapolated into the future. The main reasons are that present-day cranes could reach their capacity limit and waiting times for adequate berthing areas increase with increasing vessel dimensions. . Lian et al. (2019) note that the competition among container ship ports leads to an adaptation of infrastructure not completely reflected within the prices charged for shipping companies. An upper bound of ship size corresponding to a capacity of 26,000 to 30,000 TEU is identified, resulting from the extrapolation of freight demands. It can be summarized that the global trend of increasing ship dimensions might have not yet reached its peak. A survey among experts on the shipping industry concludes that further development of container ship size mainly depends on the development of infrastructure comprising port infrastructure, and port accessibility within the next 20 years (Gomez Paz et al., 2015).

Alongside with the global development of ship sizes, local adaptation measures are taking place in order to allow the ships, currently in operation, to enter ports restricted in their accessibility to date. As a consequence, the Elbe estuary for example is currently subject to dredging activities, making the port of Hamburg accessible to ships with a draft up to 14.5 m (WSV, 2021*a*). Similar adaptation works of access channels are also realized at Charleston Harbour (South Carolina Ports Authority, 2021), New York/New Jersey Harbour (U.S. Army Corps of Engineers, 2019), or Jacksonville Harbour (Jacksonville Port Authority, 2021). The adaptation of the Panama Canal locks to accommodate larger ships, formerly a bottleneck on ship sizes, intensified the demand for deep draft harbours (Park et al., 2020). Further remarks on future dredging projects improving port accessibility focusing on southeastern United States are given by Carse and Lewis (2020). The authors highlight the need for an interdisciplinary evaluation of the balance of economical impact and environmental and social costs that come with dredging projects.

The deepening of waterways leads to a reduction of primary wave height, if the dimensions of ships navigating on them remains constant, as the blockage coefficient is reduced. However, it can be anticipated that increasingly large ships will use the adapted waterways. This results in higher blockage and reduced distance to the shoreline, known to intensify wave loads by ship-generated wakes. In addition to maximum vessel size at a specific port, navigation frequency of large ships accessing ports is increasing (Stastistisches Bundesamt, 2018; UNCTAD, 2020). This results in higher frequency of primary wave induced loads, contributing to damage of estuarine infrastructure.

In addition, further adaptations of port accessibility do not only focus on enabling larger ships to enter a port but also to cater for the densification of traffic intensity, illustrated by means of example in Figure 8. Currently ongoing adaptation measures to access the port of Hamburg include the construction of an encountering zone where ships with a cumulative width of 104 m can encounter (WSV, 2021*b*). Even though not intensely studied to date, it is known that squat magnitudes increase when ships encounter in confined waterways, due to the further acceleration of return flows associated with higher blockage coefficients (Gourlay, 2009; Briggs et al., 2010). On this basis, it can be concluded that drawdown waves equally increase in their amplitude in case of ship encounter. The propagation of this superposition of drawdown waves generated by two ships into the waterway remains a topic of further research.

Summarizing the findings of this section it can be concluded that, despite the uncertainty in predicting the future development of maritime freight traffic, several indicators suggest that primary wave induced loads are likely to continue intensifying on coastal waterways in a mid term future. The presumed increasing size of ships travelling through confined waters and higher traffic intensity, resulting in more frequent occurrence of drawdown waves, are the main drivers for the expected development. In addition, ship encounters can be anticipated to become more frequent, potentially leading to larger superimposed drawdown wave heights.

5.1.2 Environmentally friendly bank protection measures

Environmentally friendly bank protection measures, replacing traditional riprap, are known to be beneficial for waterways in terms of the chemical attributes of water quality compared to classic technical solutions (Symmank et al., 2020). They may serve as one component in the overall restoration of rivers and estuaries along with the removal of barriers and the generation of structural areas serving as habitats within waterways (Feld et al., 2011). However, regardless of the generally beneficial effect of nature-based solutions, they should be carefully chosen for each specific site to provide the largest possible benefit (Palmer et al., 2005). It was highlighted in Section 3 that ship-generated primary waves exert remarkable loads on confined waterways, warranting solid engineering knowledge to assure safe and stable design solutions.

Removing embankment protection measures at the Meuse River, in order to contribute to the ecological value of the river by allowing erosion, amplifies the effect of primary waves on river bank erosion (Duró et al., 2020). At the site, an almost horizontal terrace of locally occurring sand is setting in next to the navigated channel, below the water surface. As primary waves were found to propagate over the local terrace, they are decisive for plant growth and the shape of the terrace. Floods are found to erode upper banks, where erosion intensity is mainly controlled by protective plant growth. This relation highlights the complex cascading effects ship waves can have. It was further shown that such gently sloping terraces may even have an adverse effect on biologic diversity, as these areas and the species living within experience high velocities due to ship drawdown (Liedermann et al., 2014; Schludermann et al., 2014).

Several measures to dampen ship waves were already tested. The construction of tidal fences, composed of recycled Christmas trees, in an estuarine region of the Mississipi River reduces wave energy, including ship wave components, by about 50 % and is, therefore, considered beneficial for restricting erosion at the site (Boumans et al., 1997). Brush bundles were observed to efficiently damp secondary waves generated by boats in an estuarine environment (Ellis et al., 2002). Several different strategies of dampening recreational boat generated waves and reduce induced erosion within an estuarine environment are presented by Herbert et al. (2018). A measure, tested to overcome primary wave induced erosion in a navigated river, consists of wooden piles, positioned at cut banks. This strategy intends to provide a sheltered area, allowing plant growth behind, introducing a second layer of wave damping mechanisms, while, at the same time, providing a valuable habitat. Field measurements have been performed at the river Lys, Belgium, to determine the effect of ship waves on banks protected by this type of installation. The comparison of the water level time series for gauges in front and behind the construction indicates no significant reduction resulting from the piles. The steepening of the drawdown's rear slope, characteristic to ship-generated drawdown waves, is observed at this site as well (de Roo and Troch, 2013). An analysis of bank retreat over 1 year, for banks with and without protection at river Lys, did not suggest any positive impact with regard to ship wave induced loads (de Roo and Troch, 2015). The installation of fascines and live willow revetments on banks subject to intensive primary wave loads, but already partly protected by a rock training dam, within the Elbe estuary suggest promising effect on erosion stability at the site (Gätje et al., 2018). A large variety of further measures introduced at the German estuaries are compiled in (BAW, 2020), typically carried out in lower load settings. However, examples from banks along the main shipping routes (e.g. Elbe, Weser) show that bio-engineered structures can indeed be applied along heavily trafficked waterways. Little rigorous analysis regarding long-term stability of these structures has been carried out to date though. Yet, experience suggests that the maintenance effort can be considerably higher than rock structures.

The shipping fleet travelling a waterway determines the intensity of local loads, rendering the inclusion of ship-induced effects necessary in the design of nature-based solutions. Introducing nature-based solutions might be beneficial from a perspective of the waterway's maintenance for navigation and its ecological value alike, considering the damaging effects of primary waves on unprotected banks and habitats, as highlighted in Sections 3.1 and 3.3. The flexibility and possibilities to combine several nature-based solutions, provides a promising perspective to enhance the stability of waterways against ship-induced loads and to increase the ecological value of waterways. However, it can be assumed that nature-based solutions themselves are prone to damage caused by ship-induced primary waves, such as in the severe impact showcased in Section 3. Design guidelines for nature-based solutions for the embankments of inland waterways are already elaborated on by Söhngen et al. (2018) and include ship-induced loads. However, the authors emphasize the relatively narrow parameter space studied and the neglection of measures in front of the banks to dampen wave energy before load is induced on the revetments.

In coastal waterways, naturally induced loads arising from exposition to wind-generated waves, tides and storm surges result in higher stress acting upon the embankments. The conjunction of natural loads with additionally occurring remarkable ship-induced loads suggests more complex impact on coastal shoreline stability in response to wave interaction of various origin. Few scientific data exists on the impact of ecological engineering measures on the long-term stability of the banks they protect. Present-day solutions are to some extent based on practical experience, rather than exact quantification of the interrelation of loads and embankment stability.

Thus, further research is required allowing the detailed prediction of ship-generated wave characteristics to determine the loads on innovative revetments, allowing a detailed assessment of their capabilities and limitations. This involves studying nature-based solutions in the load climate of coastal waterways as exemplified in Figure 9 and to assess further measures for dampening wave energy in inland waterways.

5.1.3 Future research questions resulting from-ship waves and their superposition with ambient conditions

It is known that the environmental conditions during the navigation influence the impact of ship waves. In tidal waterways, the water level varies with the tides or possible storm surges. While a determining effect of tidal water level was already found for the hydrodynamic loading on groynes (Melling et al., 2019) and tidal gates (Uliczka et al., 2009), it is reasoned that it can be similarly relevant for loading on other structures. Thus, this interrelation between water level and ship-induced loads requires further research. In addition, sea level rise will further modify estuary hydrodynamics and thus change the ambient conditions during navigation. The

Figure 8: Traffic intensification leads to a high frequency in ship-generated wave loading, as well as the superposition of effects from encountering or overtaking ships as shown here for the Kiel Canal. (Source: German Federal Waterways Engineering and Research Institute).

Figure 9: Nature based erosion defences like this gabion-filled wooden stake piling and brushwood mattresses need to withstand ship-induced loading. (Source: German Federal Waterways Engineering and Research Institute).

resulting effect - regarding the location of the still water-level or the altered waterway cross-sections for instance - could further challenge the existing methods for ship-induced wave prediction. Prognostic methods for the future sea level exist (e.g. Fox-Kemper et al. (2021)). Yet, methods need to be found that combine different scenarios for future sea-level rise with prediction methods for ship-induced loads.

For inland waterways, changing flow regimes may similarly cause interdependencies between the current water level and the ship-induced loading. The water level not only depends on the hydrological discharge regime but is further influenced by anthropogenic river control structures, such as dams and hydropower plants. In addition to their influence on the water level, these measures affect the sediment balance of rivers, ultimately affecting river cross-sections. It was already intensively discussed that bathymetric attributes influence the propagation of ship-generated waves. Hence, the determination of ship-induced loads with respect to the position of a given study site relative to river control structures requires further research, that should also consider the temporal evolution of the sediment balance.

Both types of waterways, inland and tidal ones, are subject to currents of different origin. For wind waves it is known, that the superposition of waves and currents, lead to a cascade of complex effects, including a change of wave kinematics (Hashemi et al., 2016; Zhang et al., 2022). For ship waves, this interrelation was not studied yet, but in the future this should equally be a subject of research.

5.2 Opportunities arising from advances in depth-averaged phase-resolved numerical wave modelling

In the following, some remarks are given on how advances from numerical modelling techniques can contribute to help to solve the future challenges noted in Section 5.1. Depth-averaged models, based on either the Boussinesq equations or SWE, are subject to continued development, yielding more accurate and efficient codes. The inclusion of ship structures via a pressure term, as widely applied for the depth-averaged methods (see Section 4.2.3), provides the ability to include ships via a relatively simple adaptation of the code. Therefore, recent improvements of this type of numerical models are summarized in the following paragraphs, irrespective of whether the generation of ship waves is already included in the respective code.

Brocchini (2013) summarizes the advances of the developments of Boussinesq equations for practical purposes in coastal engineering. The application range of the models based on Boussinesq equation and SWE converges to each other, due to the latest advances in modelling. Boussinesq equations, known to be precise for the prediction of processes on a coastal scale, are being improved in terms of computational efficiency. The more efficient SWE tools are being improved in terms of their description of actual wave physics by adding nonlinear terms to the governing set of equations. Boussinesq equations collapse into shallow-water-equations when dispersion characteristics are neglected (Jeschke et al., 2017). On the other hand, the inclusion of non-hydrostatic pressure approximation in SWE tools results in the additional inclusion of dispersion characteristics of the solution (Jeschke et al., 2017).

Advances in tools relying on SWE comprise the use of a multi layer approach and non-hydrostatic pressure assumption, as presented by Stelling and Zijlema (2003); Jeschke et al. (2017). Further increase in efficiency is obtained by vertically splitting the domain into a hydrostatic and a non-hydrostatic layer, yielding a tool capable of wave prediction in shallow and intermediate water depths (de Ridder et al., 2021). The simpler mathematical description of vertical flow components within SWE compared to Boussinesq equations can further be compensated introducing high order numerical discretization schemes (Wang et al., 2020*b*). Further advances include the modelling of parametric wave breaking (Smit et al., 2013) and the introduction of unstructured meshes within a non-hydrostatic solver (Zijlema, 2020).

Similarly, parallelization was also introduced to Boussinesq type models, yielding a more efficient simulation tool (Shi et al., 2012). Solving the Boussinesq equations on multiple Graphics Processing Units (GPU) is further reported to contribute to the efficiency of Boussinesq tools (Yuan et al., 2020). Comparison of a Boussinesq and a SWE tool shows that the results of solitary wave run up on a slope almost identical, if no wave breaking is expected (Liang et al., 2013).

Furthermore, coupling between numerical models of different accuracy and dynamically adaptive meshing (Beisiegel et al., 2020) has proved to be efficient by shifting the computational demand only into the regions where high accuracy is required. Coupling might either be done in the form of one-way coupling, ensuring information exchange just from one model to the other. Bi-directional, or two-way, coupling pursues a mutual exchange between both models involved. Examples for coupling potential flow theory based codes in the far field with RANSE solvers for the near field are given in Biausser et al. (2004); Lu et al. (2016); Paulsen et al. (2014); Vukcevic (2016); Li et al. (2018, 2019); Choi (2019); Musiedlak et al. (2020).

Di Paolo et al. (2020) suggest to couple one and two dimensional domains in RANSE solvers. Other variations of numerical coupling are given by Verbrugghe et al. (2018), coupling a potential flow based model to Smoothed particle hydrodynamics (SPH), by Janßen et al. (2010) for coupling a potential flow based model to a particle based Lattice-Boltzman method, and by Mintgen (2018) for coupling a SWE tool to a 3D RANSE solver. As introduced in Section 4, Bellafiore et al. (2018) suggested to couple a CFD code to a SWE code. Due to the disparate needs regarding the computational domain for predicting the far field propagation of ship-generated drawdown waves and locally required accuracy, such coupling schemes appear to be promising methods to address future challenges.

The balance of provided accuracy and relative efficiency of numerical tools based on Boussinesq equations or SWE allows the calculation of phase-resolved wave propagation on a relatively large scale of real coastal, estuarine or river bathymetries. Ship-generated primary waves are known to deform during their propagation. Therefore, the inclusion of local bathymetric influences is indispensable to accurately predict primary wave induced loads on a specific location at the coast. In shallow areas of river banks the deformation processes are known to cause breaking of the drawdown rear slope. Furthermore, vertical velocity components are identified, resulting from primary waves in very shallow water. The interaction of the drawdown wave with rough structures like riprap and rock structures like groins, can be expected to include turbulent interaction processes. Furthermore, waves approaching banks are known to cause complex current conditions, including opposing currents at different vertical layers of the water-column (Elsayed et al., 2022). Due to the model limitations, such vertically in-homogeneous or turbulent processes can not be replicated by a depth-averaged model. High fidelity models based on RANSE can likely predict the mentioned three-dimensional turbulent processes (Fleit et al., 2016, 2019).

Hence, a coupled approach relying on a depth-averaged model coupled to a CFD-code is expected to be able to predict the relevant process cascade with the required level of detail. Primary wave-generation and wave propagation over a complex bathymetry can be simulated using the depth-averaged model. Where three-dimensional processes are expected to be of relevant magnitude, further simulations performed with a CFD code can provide sufficient accuracy for load prediction. The resulting site-specific hydrodynamic data of local velocities and pressure is highly spatially resolved and may therefore be used to answer questions regarding structural stability, morphodynamics, and ecological concerns alike. The limited guidance for the design of engineering structures subject to primary wave loads can be complemented by bathymetric-sensitive numerical models in order to predict the effect of design decisions.

6 Conclusions

This review work has focused on long-period, primary waves originating from ships and vessels sailing in confined water, highlighting the need to conduct further research into this neglected aspect of river and estuary engineering. On the basis of the comprehensive literature review of the loads and effects of these long waves, our work has outlined the relevance of primary-waves compared to other ship-generated wave systems. The following conclusions, with respect to the topic at hand, can be drawn and future research demands be outlined:

- Large ships progressing through confined waterways generate long-period drawdown waves of significant, often design-relevant magnitude. While the generation of primary waves is considered in the design of embankment protection measures of inland waterways, the impact of drawdown waves in larger coastal waterways remain largely neglected. Key publications suggest that the induced loads are already considerably impacting morphology, structures and ecologic habitats. Confinement is an attribute defined by the relative dimensions of ship and waterway. With growing ship dimensions waterways previously considered to exhibit only moderate confinement, now become subject to intense primary wave loads. Sea-going ships' size can be assumed to increase in a midterm future, presumably resulting in more intense drawdown wave generation and thus loading on the surrounding waterway. Hence, ship-induced loads need to be routinely considered when making design decisions on waterways subject to marine traffic.
- Adding ecological value to waterways often includes establishing shallow areas at river banks, replacing riprap with innovative nature-based revetments or installing additional layers of wave-dampening measures. Improving the ecological value of embankments along rivers and estuaries is a decadal challenge that will have to be given much consideration, and therefore, guidance and engineering knowledge will become key to a successful transition. Given these more complex bathymetric features, ship-generated drawdown waves deform substantially during their propagation analogous to the effects observed in coastal waterways. The loads induced by a propagating drawdown wave can hence be expected to vary largely at different locations of the waterway, dependent on the stage of wave transformation within the bathymetry surrounding a ship. Hence, methods are required that are able to predict drawdown wave characteristics, spatially-resolved to be able to determine the resulting local loads. Besides providing input data for the structural design, this information might further be beneficial for quantifying the impact on local plants and animals, sparking research on management strategies to reduce the ecological impact of shipping traffic in both coastal and inland waterways.
- Different from the assumed cross-sections in empirical equations and existing design guidelines for waterway embankment design, rivers and coastal waterways can only partly be described by the assumption of a constant cross-section. Consequently, the guidance needs to be updated to account for the complex deformation processes during drawdown wave propagation in non-constant waterway cross-sections of inland waterways. Further, the larger dimensions of ships and waterways make the development of specific guidelines for coastal waterway design in response to ship-induced loads necessary, based upon existing design standards for inland waterways. In addition, structural elements of waterways such as groins subject to overtopping are not covered sufficiently by present day guidelines. Experimental tests allowed for the adaption of groin design for one specific site. The adapted geometry is found to withstand the new loads induced by the present-day navigation fleet. Yet, the development of design guidance based on these findings is required, for designing groins at varying locations, subject to loads induced by a different navigation fleet. Furthermore, in addition to structural stability, the provision of ecologic benefit is of increasing importance. Hence, this aspect needs consideration while developing design criteria, putting nature-based revetment solution into the focus of future research.
- Empirical and analytical approaches are not fully suitable to include the multivariate input data arising from complex bathymetries in sufficient detail. Therefore they are limited to modified waterways, or require site-specific input data from experimental data or field measurements. In the past, depth-averaged numerical methods proved successful in predicting drawdown wave propagation in real-world bathymetries. In addition, in the last decade computational efficiency and accuracy of SWE-models has been further improved, allowing a precise phase-resolved wave simulation of kilometer-scale spatial domains. However, the inherent assumptions limit the application to highly spatially resolved processes taking place on waterway banks. This drawback can be overcome by coupling a depth-averaged model to a RANSE-CFD code, computationally too demanding to apply it to the entire domain, detailing the 3D-processes on a

small scale. Information exchange between the models can be established by implementing a one-way-coupling. Exploiting the advances in numerical modelling in such a way can help defining the required design guidelines for structures within coastal waterways and natural or renaturalized inland waterways alike.

Acknowledgements

This study is part of the research project NumSiSSI (Numerical Simulation of Shipwave-Structure-Interaction in Coastal Areas) conducted in cooperation with the German Federal Waterways Engineering and Research Institute (BAW).

Author contributions

L-CD: Writing-original draft, Visualization; GM: Project planning, Manuscript draft review and editing, Conceptualization; CW: Manuscript draft review and editing; OL: Manuscript draft review and editing, Conceptualization; TM: Manuscript draft review and editing, Conceptualization; IH: Project planning, Conceptualization, Manuscript Draft Review; HB: Conceptualization, Manuscript Draft Review; NG: Project planning, Conceptualization, Manuscript Draft Review.

Acronyms

AIS	Automatic Identification System
BEM	Boundary-element-method
CFD	Computational fluid dynamics
GPU	Graphics Processing Unit
RANSE	Reynolds-averaged Navier-Stokes equations
SPH	Smoothed particle hydrodynamics
SPM	Suspended particulate matter
SSC	Suspended Sediment Concentration
SWE	Shallow-water-equations
TEU	Twenty-foot equivalent Unit

Notation

A_C	Waterway cross-section
A_S	Ship cross-section
B	Ship beam
D	Ship draft
d	Distance ship shoreline
F_h	Depth Froude-Number
g	Gravitational acceleration
h	Water depth
L	Ship length
r	Hydraulic mean-depth
S	Channel blockage coefficient

C_B Ship block coefficient
T Waterway top width
V Ship speed

References

Abbasnia, A. and Soares, C.G. (2019). Fully nonlinear and linear ship waves modelling using the potential numerical towing tank and nurbs. *Engineering Analysis with Boundary Elements*, **103**, 137–144. ISSN 09557997. doi:10.1016/j.enganabound.2019.03.009.

Adams, S.R., Keevin, T.M., Killgore, K.J. and Hoover, J.J. (1999). Stranding potential of young fishes subjected to simulated vessel-induced drawdown. *Transactions of the American Fisheries Society*, **128**(6), 1230–1234. ISSN 0002-8487.

Alderf, N., Lefrançois, E., Sergent, P. and Debaillon, P. (2011). Dynamic ship response integration for numerical prediction of squat in highly restricted waterways. *International Journal for Numerical Methods in Fluids*, **65**(7), 743–763. ISSN 0271-2091. doi:10.1002/fld.2194.

Ali, M.M., Murphy, K.J. and Langendorff, J. (1999). Interrelations of river ship traffic with aquatic plants in the river nile, upper egypt. *Hydrobiologia*, **415**(0), 93–100. ISSN 0018-8158. doi:10.1023/A:1003829516479.

Almström, B. and Larson, M. (2020). Measurements and analysis of primary ship waves in the stockholm archipelago, sweden. *Journal of Marine Science and Engineering*, **8**(10), 743. doi:10.3390/jmse8100743.

Almström, B., Roelvink, D. and Larson, M. (2021). Predicting ship waves in sheltered waterways – an application of xbeach to the stockholm archipelago, sweden. *Coastal Engineering*, **170**, 104026. ISSN 03783839. doi:10.1016/j.coastaleng.2021.104026.

B. Bauer, M. S. Lorang and D. Sherman (2002). Estimating boat-wake-induced levee erosion using sediment suspension measurements. *Journal of Waterway, Port, Coastal, and Ocean Engineering*, **128(4)**. ISSN 0733-950X.

Barrass, C.B. and Derrett, D.R. (Editors) (2013). *Ship stability for masters and mates*, Butterworth-Heinemann, Oxford, 7. ed., transferred to digital printing edition.

BAW (2010). Principles for the design of bank and bottom protection for inland waterways (gbb): Code of practice federal waterways engineering and research institute of germany karlsruhe, germany. https://izw.baw.de/publikationen/merkblaetter/0/BAWCodeofPractice_Principles_Bank_Bottom_Protection_Inland_Waterways_GBB_2010.pdf.

BAW (2016). Driving dynamics of inland vessels: Vessel behaviour on european inland waterways and waterway infrastructure with special respect to german waterways: https://izw.baw.de/publikationen/pianc/0/BAW_VBW_Driving_Dynamics_of_Inland_Vessels.pdf.

BAW (2018). Schiffserzeugte langperiodische belastung zur bemessung der deckschichten von strombauwerken an seeschifffahrtsstraßen: https://www.baw.de/content/files/forschung_entwicklung/documents/B3955.02.04.70141.pdf.

BAW (2020). Living shoreline techniques along estuarine waterways - an overview of all measures: https://ufersicherung-baw-bfg.baw.de/aestuarbereich/en/massnahmen.

BBC (2021). The cost of the suez canal blockage: - last access: 1.2.2022: https://www.bbc.com/news/business-56559073. *BBC News*.

Bechthold, J. and Kastens, M. (2019). Robustness and quality of squat predictions in shallow water conditions based on rans-calculations. *Proceedings of the 5th International Conference on Ship Manoeuvring in Shallow and Confined Water (MASHCON), 19 – 23 May 2019, Ostend, Belgium*, 11–24.

Bechthold, J. and Kastens, M. (2020). Robustness and quality of squat predictions in extreme shallow water conditions based on rans-calculations. *Ocean Engineering*, **197**, 106780. ISSN 00298018. doi:10.1016/j.oceaneng.2019.106780.

Beck, R.F., Newman, J.N. and Tuck, E.O. (1975). Hydrodynamic forces on ships in dredged channels. *Journal of Ship Research*, **19**(03), 166–171. ISSN 0022-4502. doi:10.5957/jsr.1975.19.3.166.

Beisiegel, N., Vater, S., Behrens, J. and Dias, F. (2020). An adaptive discontinuous galerkin method for the simulation of hurricane storm surge. *Ocean Dynamics*, **70**(5), 641–666. ISSN 1616-7341. doi:10.1007/s10236-020-01352-w.

Beji, S. and Nadaoka, K. (1996). A formal derivation and numerical modelling of the improved boussinesq equations for varying depth. *Ocean Engineering*, **23**(8), 691–704. ISSN 00298018. doi:10.1016/0029-8018(96)84408-8.

Bellafiore, D., Zaggia, L., Broglia, R., Ferrarin, C., Barbariol, F., Zaghi, S., Lorenzetti, G., Manfè, G., de Pascalis, F. and Benetazzo, A. (2018). Modeling ship-induced waves in shallow water systems: The venice experiment. *Ocean Engineering*, **155**, 227–239. ISSN 00298018. doi:10.1016/j.oceaneng.2018.02.039.

Bertram, V. (2002). *Practical ship hydrodynamics*, Butterworth-Heinemann, Oxford, reprint edition.

Bhowmik, N.G., Demissie, M. and Osakada, S. (1981). Waves and drawdown generated by river traffic on the illinois and mississippi rivers: Sws contract report 271: https://www.isws.illinois.edu/pubdoc/CR/ISWSCR-271.pdf.

Biausser, B., Fraunié, P., Grilli, S. and Marcer, R. (2004). Numerical analysis of the internal kinematics and dynamics of three-dimensional breaking waves on slopes. *International Journal of Offshore and Polar Engineering*, **14**(4), 247–256. ISSN 1053-5381.

Bilkovic, D.M., Mitchell, M.M., Davis, J., Herman, J., Andrews, E., King, A., Mason, P., Tahvildari, N., Davis, J. and Dixon, R.L. (2019). Defining boat wake impacts on shoreline stability toward management and policy solutions. *Ocean & Coastal Management*, **182**, 104945. ISSN 0964-5691. doi:10.1016/j.ocecoaman.2019.104945.

Blaauw, H.G. and van der Knaap, F. (1983). Prediction of squat of ships sailing in restricted water. *In the proceedings of 8th International Harbour Congress, Antwerpen, Belgium.*

Boumans, R.M., Day, J.W., Kemp, G. and Kilgen, K. (1997). The effect of intertidal sediment fences on wetland surface elevation, wave energy and vegetation establishment in two louisiana coastal marshes. *Ecological Engineering*, **9**(1-2), 37–50. ISSN 09258574. doi:10.1016/S0925-8574(97)00028-1.

Braga, F., Scarpa, G.M., Brando, V.E., Manfè, G. and Zaggia, L. (2020). Covid-19 lockdown measures reveal human impact on water transparency in the venice lagoon. *The Science of the total environment*, **736**, 139612. doi:10.1016/j.scitotenv.2020.139612.

Briggs, M., Vantorre, M., Uliczka, K. and Debaillon, P. (2010). Prediction of squat for underkeel clearance, In: Young C. Kim (Editor), *Handbook of Coastal and Ocean Engineering*, 723–774, World Scientific.

Briggs, M.J. (2006). Ship squat predictions for ship/tow simulator: Usace technical report: https://apps.dtic.mil/sti/pdfs/ADA454654.pdf.

Brocchini, M. (2013). A reasoned overview on boussinesq-type models: the interplay between physics, mathematics and numerics. *Proceedings. Mathematical, physical, and engineering sciences*, **469**(2160), 20130496. ISSN 1364-5021. doi:10.1098/rspa.2013.0496.

Byrnes, T.A. and Dunn, R.J.K. (2020). Boating- and shipping-related environmental impacts and example management measures: A review. *Journal of Marine Science and Engineering*, **8**(11), 908. doi:10.3390/jmse8110908.

Carse, A. and Lewis, J.A. (2020). New horizons for dredging research: The ecology and politics of harbor deepening in the southeastern united states. *WIREs Water*, **7**(6), e1485. ISSN 2049-1948. doi:10.1002/wat2.1485.

Chen, X., Zhu, R., Ma, C. and Fan, J. (2016). Computations of linear and nonlinear ship waves by higher-order boundary element method. *Ocean Engineering*, **114**, 142–153. ISSN 00298018. doi:10.1016/j.oceaneng.2016.01.016.

Chen, X.N. and Sharma, S.D. (1995). A slender ship moving at a near-critical speed in a shallow channel. *Journal of Fluid Mechanics*, **291**, 263–285. ISSN 1469-7645. doi:10.1017/S0022112095002692.

Chi, Y. and Huang, F. (2016). An overview of simulation-based hydrodynamic design of ship hull forms. *Journal of Hydrodynamics, Ser. B*, **28**(6), 947–960.

Choi, Y. (2019). *Two-way Coupling between Potential and Viscous Flows for a Marine Application*, Ph.d thesis, École Centrale de Nantes.

Ciortan, C., Wanderley, J. and Soares, C.G. (2012). Free surface flow around a ship model using an interface-capturing method. *Ocean Engineering*, **44**, 57–67. ISSN 00298018. doi:10.1016/j.oceaneng.2012.01.015.

CIRIA (2007). The rock manual. the use of rock in hydraulic engineering. *CIRIA-CUR, Publication C683*.

CNN (2020). Venice's canal water looks clearer as coronavirus keeps visitors away: https://edition.cnn.com/travel/article/venice-canals-clear-water-scli-intl/index.html: -last access: 20.01.22.

Constantine, T. (1960). On the movement of ships in restricted waterways. *Journal of Fluid Mechanics*, **9**(2), 247–256. ISSN 1469-7645. doi:10.1017/S0022112060001080.

Cullinane, K. and Khanna, M. (1999). Economies of scale in large container ships. *Journal of Transport Economics and Policy*, **33**(Part 2), 185–208.

Dam, K.T., Tanimoto, K. and Fatimah, E. (2008). Investigation of ship waves in a narrow channel. *Journal of Marine Science and Technology*, **13**(3), 223–230. ISSN 0948-4280. doi:10.1007/s00773-008-0005-6.

Dand, I.W. and White, W.R. (1978). Design of navigation canals, In: *2nd Symposium, Aspects of Navigability of Constraint Waterways; Including Harbour Entrances*.

Dauphin, D. (2000). *Influence de la navigation commerciale et de la navigation de plaisance sur l'érosion des rives du Saint-Laurent dans le tronçon Cornwall - Montmagny : Rapport final*, Service du transport maritime et aérien.

David, C.G., Roeber, V., Goseberg, N. and Schlurmann, T. (2017). Generation and propagation of ship-borne waves - solutions from a boussinesq-type model. *Coastal Engineering*, **127**, 170–187. ISSN 03783839. doi:10.1016/j.coastaleng.2017.07.001.

Davis, S.E., Allison, J.B., Driffill, M.J. and Zhang, S. (2009). Influence of vessel passages on tidal creek hydrodynamics at aransas national wildlife refuge (texas, united states): Implications on materials exchange. *Journal of Coastal Research*, **252**(252), 359–365. ISSN 1551-5036. doi:10.2112/07-0946.1.

Dawson, C.W. (1977). A practical computer method for solving ship-wave problems, In: *Proceedings of Second International Conference on Numerical Ship Hydrodynamics*, 30–38.

de Jong, M.P.C., Roelvink, D., Reijmerink, B. and Breederveld, C. (2013). Numerical modelling of passing-ship effects in complex geometries and on shallow water, In: P. Rigo and M. Wolters (Editors), *the proceedings of Pianc Smart Rivers 2013, Liege, Maastricht*.

de Ridder, M.P., Smit, P.B., van Dongeren, A.R., McCall, R.T., Nederhoff, K. and Reniers, A.J. (2021). Efficient two-layer non-hydrostatic wave model with accurate dispersive behaviour. *Coastal Engineering*, **164**, 103808. ISSN 03783839. doi:10.1016/j.coastaleng.2020.103808.

de Roo, S. and Troch, P. (2013). Field monitoring of ship wave action on environmentally friendly bank protection in a confined waterway. *Journal of Waterway, Port, Coastal, and Ocean Engineering*, **139**(6), 527–534. ISSN 0733-950X. doi:10.1061/(ASCE)WW.1943-5460.0000202.

de Roo, S. and Troch, P. (2015). Evaluation of the effectiveness of a living shoreline in a confined, non-tidal waterway subject to heavy shipping traffic. *River Research and Applications*, **31**(8), 1028–1039. ISSN 1535-1459. doi:10.1002/rra.2790.

Denehy, S.P., Duffy, J.T., Ranmuthugala, D. and Renilson, M.R. (2016). Squat in berthed ship - passing ship interaction for restricted water cases, In: Klemens Uliczka, Carl-Uwe Böttner, Marko Kastens, Katrien Eloot, Guillaume Delefortrie, Marc Vantorre, Maxim Candries, Evert Lataire (Editor), *in the proceedings of 4th MASHCON*, Bundesanstalt für Wasserbau, Karlsruhe.

Di Paolo, B., Lara, J.L., Barajas, G. and Losada, Í.J. (2020). Wave and structure interaction using multi-domain couplings for navier-stokes solvers in openfoam®. part i: Implementation and validation. *Coastal Engineering*, 103799. ISSN 03783839. doi:10.1016/j.coastaleng.2020.103799.

Didenkulova, I., Pelinovsky, E. and Soomere, T. (2011). Can the waves generated by fast ferries be a physical model of tsunami? *Pure and Applied Geophysics*, **168**(11), 2071–2082. ISSN 0033-4553. doi:10.1007/s00024-011-0289-z.

Dogrul, A., Song, S. and Demirel, Y.K. (2020). Scale effect on ship resistance components and form factor. *Ocean Engineering*, **209**, 107428. ISSN 00298018. doi:10.1016/j.oceaneng.2020.107428.

Dong, G.H., Sun, L., Zong, Z. and Zhao, Y.P. (2009). Numerical analysis of the forces exerted on offshore structures by ship waves. *Ocean Engineering*, **36**(6-7), 468–476. ISSN 00298018. doi:10.1016/j.oceaneng.2009.01.012.

Du, P., Ouahsine, A., Sergent, P. and Hu, H. (2020). Resistance and wave characterizations of inland vessels in the fully-confined waterway. *Ocean Engineering*, **210**, 107580. ISSN 00298018. doi:10.1016/j.oceaneng.2020.107580.

Duró, G., Crosato, A., Kleinhans, M.G., Roelvink, D. and Uijttewaal, W.S.J. (2020). Bank erosion processes in regulated navigable rivers. *Journal of Geophysical Research: Earth Surface*, **125**(7). ISSN 2169-9003. doi:10.1029/2019JF005441.

El Safty, H. and Marsooli, R. (2020). Ship wakes and their potential impacts on salt marshes in jamaica bay, new york. *Journal of Marine Science and Engineering*, **8**(5), 325. doi:10.3390/JMSE8050325.

Ellis, J., Sherman, D., Bauer, B. and Hart, J. (2002). Assessing the impact of an organic restoration structure on boat wake energy. *Journal of Coastal Research*, **36**. ISSN 0749-0208.

Elsayed, S.M., Gijsman, R., Schlurmann, T. and Goseberg, N. (2022). Nonhydrostatic numerical modeling of fixed and mobile barred beaches: Limitations of depth-averaged wave resolving models around sandbars. *Journal of Waterway, Port, Coastal, and Ocean Engineering*, **148**(1). ISSN 0733-950X. doi:10.1061/(ASCE)WW.1943-5460.0000685.

Elsherbiny, K., Terziev, M., Tezdogan, T., Incecik, A. and Kotb, M. (2020). Numerical and experimental study on hydrodynamic performance of ships advancing through different canals. *Ocean Engineering*, **195**, 106696. ISSN 00298018. doi:10.1016/j.oceaneng.2019.106696.

Elsherbiny, K., Tezdogan, T., Kotb, M., Incecik, A. and Day, S. (2019). Experimental analysis of the squat of ships advancing through the new suez canal. *Ocean Engineering*, **178**, 331–344. ISSN 00298018. doi:10.1016/j.oceaneng.2019.02.078.

Erm, A. and Soomere, T. (2004). Influence of fast ship waves on the optical properties of sea water in tallinn bay, baltic sea, In: *Proceedings of the Estonian Academy of Sciences, Biology and Ecology*, volume 53, 161–178.

Ersan, D.B. and Beji, S. (2013). Numerical simulation of waves generated by a moving pressure field. *Ocean Engineering*, **59**, 231–239. ISSN 00298018. doi:10.1016/j.oceaneng.2012.12.025.

Ertekin, R.C., Webster, W.C. and Wehausen, J.V. (1986). Waves caused by a moving disturbance in a shallow channel of finite width. *Journal of Fluid Mechanics*, **169**(-1), 275. ISSN 0022-1120. doi:10.1017/S0022112086000630.

Feld, C.K., Birk, S., Bradley, D.C., Hering, D., Kail, J., Marzin, A., Melcher, A., Nemitz, D., Pedersen, M.L., Pletterbauer, F., Pont, D., Verdonschot, P.F. and Friberg, N. (2011). Chapter three - from natural to degraded rivers and back again: A test of restoration ecology theory and practice, In: G. Woodward (Editor), *Advances in Ecological Research*, volume 44, 119–209, Academic Press.

Fenical, S., Kolomiets, P., Kivva, S. and Zheleznyak, M. (2007). Numerical modeling of passing vessel impacts on berthed vessels and shoreline, In: J.M. Smith (Editor), *Coastal engineering 2006*, 1234–1246, World Scientific, Singapore.

Ferziger, J.H. and Perić, M. (2002). *Computational Methods for Fluid Dynamics*, Springer Berlin Heidelberg, Berlin, Heidelberg and s.l., third, rev. edition edition.

Fleit, G. and Baranya, S. (2021). Acoustic measurement of ship wave–induced sediment resuspension in a large river. *Journal of Waterway, Port, Coastal, and Ocean Engineering*, **147**(2), 04021001. ISSN 0733-950X. doi:10.1061/(ASCE)WW.1943-5460.0000627.

Fleit, G., Baranya, S., Krámer, T., Bihs, H. and Józsa, J. (2019). A practical framework to assess the hydrodynamic impact of ship waves on river banks. *River Research and Applications*, **35**(9), 1428–1442. ISSN 1535-1459. doi:10.1002/rra.3522.

Fleit, G., Baranya, S., Rüther, N., Bihs, H., Krámer, T. and Józsa, J. (2016). Investigation of the effects of ship induced waves on the littoral zone with field measurements and cfd modeling. *Water*, **8**(7), 300. ISSN 2073-4441. doi:10.3390/w8070300.

Flory, J. and Fenical, S. (2014). Quay wall influence on passing-ship induced mooring loads, In: T. Ward and B.I. Ostbo (Editors), *in the proceedings of Ports 2010*, American Society of Civil Engineers, Reston.

Flory, J.F. (2002). The effect of passing ships on moored ships, In: *In the proceedings of Prevention First 2002 Symposium*, 1–11.

Forlini, C., Qayyum, R., Malej, M., Lam, M.A.Y.H., Shi, F., Angelini, C. and Sheremet, A. (2021). On the problem of modeling the boat wake climate: The florida intracoastal waterway. *Journal of Geophysical Research: Oceans*, **126**(2). ISSN 21699275. doi:10.1029/2020JC016676.

Fox-Kemper, B., H.T. Hewitt, C. Xiao, G. Aðalgeirsdóttir, S.S. Drijfhout, T.L. Edwards, N.R. Golledge, M. Hemer, R.E., K., G. Krinner, A. Mix, D. Notz, S. Nowicki, I.S. Nurhati, L. Ruiz, J.-B. Sallée, A.B.A. Slangen and Y. Yu (2021). Ocean, cryosphere and sea level change, In: Masson-Delmotte V., P. Zhai, A. Pirani, S.L. Connors, C. Péan, S. Berger, N. Caud, Y. Chen, L. Goldfarb, M.I. Gomis, M. Huang, K. Leitzell, E. Lonnoy, J.B.R. Matthews, T.K. Maycock, T. Waterfield, O. Yelekçi, R. Yu and B. Zhou (Editors), *Climate Change 2021: The Physical Science Climate Change 2021: The Physical Science Basis. Contribution of Working Group I to the Sixth Assessment Report of the Intergovernmental Panel on Climate Change*.

Gabel, F., Lorenz, S. and Stoll, S. (2017). Effects of ship-induced waves on aquatic ecosystems. *The Science of the total environment*, **601-602**, 926–939. doi:10.1016/j.scitotenv.2017.05.206.

Garel, E., López Fernández, L. and Collins, M. (2008). Sediment resuspension events induced by the wake wash of deep-draft vessels. *Geo-Marine Letters*, **28**(4), 205–211. ISSN 1432-1157. doi:10.1007/s00367-008-0101-y.

Garrido, J., Saurí, S., Marrero, Á., Gül, Ü. and Rúa, C. (2020). Predicting the future capacity and dimensions of container ships. *Transportation Research Record: Journal of the Transportation Research Board*, **2674**(9), 177–190. ISSN 0361-1981. doi:10.1177/0361198120927395.

Gaskin, S.J., Pieterse, J., Shafie, A.A. and Lepage, S. (2003). Erosion of undisturbed clay samples from the banks of the st. lawrence river. *Canadian Journal of Civil Engineering*, **30**(3), 585–595. ISSN 0315-1468. doi:10.1139/l03-008.

Gätje, B., Appel, J. and Wöbking, C. (2018). Technisch -biologische ufersicherung auf der elbinsel hanskalbsand: Wsv technical report: https://izw.baw.de/publikationen/alu-aestuare/0/Technisch-biologische_Ufersicherung_auf_der_Elbinsel_Hanskalbsand.pdf.

Gelencser, G.J. (1977). Drawdown surge and slope protection, experimental results, In: *Proceedings of the 24th International Navigation Congress, Leningrad*.

Gelinas, M., Bokuniewicz, H., Rapaglia, J. and Lwiza, K.M. (2013). Sediment resuspension by ship wakes in the venice lagoon. *Journal of Coastal Research*, **286**, 8–17. ISSN 0749-0208. doi:10.2112/JCOASTRES-D-11-00213.1.

Gharbi, S., Valkov, G., Hamdi, S. and Nistor, I. (2010). Numerical and field study of ship-induced waves along the st. lawrence waterway, canada. *Natural Hazards*, **54**(3), 605–621. ISSN 0921-030X. doi:10.1007/s11069-009-9489-6.

Gomez Paz, M.A., Camarero Orive, A. and González Cancelas, N. (2015). Use of the delphi method to determine the constraints that affect the future size of large container ships. *Maritime Policy & Management*, **42**(3), 263–277. ISSN 0308-8839. doi:10.1080/03088839.2013.870358.

Göransson, G., Larson, M. and Althage, J. (2014). Ship-generated waves and induced turbidity in the göta älv river in sweden. *Journal of Waterway, Port, Coastal, and Ocean Engineering*, **140**(3), 04014004. ISSN 0733-950X. doi:10.1061/(ASCE)WW.1943-5460.0000224.

Gourlay, T. (2008). Slender-body methods for predicting ship squat. *Ocean Engineering*, **35**(2), 191–200. ISSN 00298018. doi:10.1016/j.oceaneng.2007.09.001.

Gourlay, T. (2009). Sinkage and trim of two ships passing each other on parallel courses. *Ocean Engineering*, **36**(14), 1119–1127. ISSN 00298018. doi:10.1016/j.oceaneng.2009.06.003.

Gourlay, T. (2011). A brief history of mathematical ship-squat prediction, focussing on the contributions of e.o. tuck. *Journal of Engineering Mathematics*, **70**(1-3), 5–16. ISSN 0022-0833. doi:10.1007/s10665-010-9435-3.

Gourlay, T. (2014). Shallowflow: A program to model ship hydrodynamics in shallow water, In: *Proceedings of the ASME 33rd International Conference on Ocean, Offshore and Arctic Engineering - 2014*, ASME, New York, NY.

Gourlay, T. and Cook, S. (2004). Flow past a ship radiating a bore in a channel. *Journal of Engineering for the Maritime Environment*, **218**(1), 31–40. doi:10.1243/147509004774048550.

Gourlay, T., Ha, J.H., Mucha, P., Uliczka, K. et al. (2015). Sinkage and trim of modern container ships in shallow water, In: *the proceedings of the 22nd Australasian Coasts & 15th Ports Conference 2015, Auckland, New Zealand*, 344.

Hammack, E.A., Smith, D.S. and Stockstill, R.L. (2008). Modeling vessel-generated currents and bed shear stresses: Usace technical report.

Haralambides, H. (2017). Globalization, public sector reform, and the role of ports in international supply chains. *Maritime Economics & Logistics*, **19**(1), 1–51. ISSN 1479-294X. doi:10.1057/s41278-017-0068-6.

Härting, A., Laupichler, A. and Reinking, J. (2009). Considerations on the squat of unevenly trimmed ships. *Ocean Engineering*, **36**(2), 193–201. ISSN 00298018. doi:10.1016/j.oceaneng.2008.10.003.

Hashemi, M.R., Grilli, S.T. and Neill, S.P. (2016). A simplified method to estimate tidal current effects on the ocean wave power resource. *Renewable Energy*, **96**, 257–269. ISSN 09601481. doi:10.1016/j.renene.2016.04.073.

Havelock, T.H. (1908). The propagation of groups of waves in dispersive media, with application to waves on water produced by a travelling disturbance. *Proceedings of the Royal Society of London. Series A, Containing Papers of a Mathematical and Physical Character*, **81**(549), 398–430. ISSN 0950-1207. doi:10.1098/RSPA.1908.0097.

He, G. and Kashiwagi, M. (2014). Time-domain analysis of steady ship-wave problem using higher-order bem. *International Journal of Offshore and Polar Engineering*, **24**(01), 1–10. ISSN 1053-5381.

Herbert, D., Astrom, E., Bersoza, A., Batzer, A., McGovern, P., Angelini, C., Wasman, S., Dix, N. and Sheremet, A. (2018). Mitigating erosional effects induced by boat wakes with living shorelines. *Sustainability*, **10**(2), 436. doi:10.3390/su10020436.

Hochstein, A. (1967). Navigation use of industrial canals. *Water Transp.*

Hong, C.B., Doi, Y. and Matsuda, H. (2005). Numerical study on breaking phenomena of ships' waves in narrow and shallow waterways. *Journal of Marine Science and Technology*, **10**(1), 11–21. ISSN 0948-4280. doi:10.1007/s00773-004-0188-4.

Houser, C. (2011). Sediment resuspension by vessel-generated waves along the savannah river, georgia. *Journal of Waterway, Port, Coastal, and Ocean Engineering*, **137**(5), 246–257. ISSN 0733-950X. doi:10.1061/(ASCE)WW.1943-5460.0000088.

Huang, F., Yang, C. and Noblesse, F. (2013). Numerical implementation and validation of the neumann–michell theory of ship waves. *European Journal of Mechanics - B/Fluids*, **42**, 47–68. ISSN 09977546. doi:10.1016/j.euromechflu.2013.05.002.

Huang, L., Li, M., Romu, T., Dolatshah, A. and Thomas, G. (2021). Simulation of a ship operating in an open-water ice channel. *Ships and Offshore Structures*, **16**(4), 353–362. ISSN 1744-5302. doi:10.1080/17445302.2020.1729595.

Jacksonville Port Authority (2021). Harbor deepening | jacksonville port authority (jaxport): https://www.jaxport.com/cargo/port-improvements/harbor-deepening/: - last access: 01.02.22.

Janßen, C., Grilli, S.T. and Krafczyk, M. (2010). Modeling of wave breaking and wave-structure interactions by coupling of fully nonlinear potential flow and lattice-boltzmann models, In: *the proceedings of 20th Offshore and Polar Engineering Conference (ISOPE)*.

Jeschke, A., Pedersen, G.K., Vater, S. and Behrens, J. (2017). Depth-averaged non-hydrostatic extension for shallow water equations with quadratic vertical pressure profile: equivalence to boussinesq-type equations. *International Journal for Numerical Methods in Fluids*, **84**(10), 569–583. ISSN 0271-2091. doi:10.1002/fld.4361.

Ji, S., Ouahsine, A., Smaoui, H. and Sergent, P. (2014). 3d numerical modeling of sediment resuspension induced by the compounding effects of ship-generated waves and the ship propeller. *Journal of Engineering Mechanics*, **140**(6), 04014034. ISSN 0733-9399. doi:10.1061/(ASCE)EM.1943-7889.0000739.

Ji, S.C., Ouahsine, A., Smaoui, H. and Sergent, P. (2012). 3-d numerical simulation of convoy-generated waves in a restricted waterway. *Journal of Hydrodynamics*, **24**(3), 420–429. ISSN 1001-6058. doi:10.1016/S1001-6058(11)60263-1.

Jiang, T. (1998). Investigation of waves generated by ships in shallow water, In: *The Proceedings of 22nd Symposium on Naval Hydrodynamics*, 601–612.

Jiang, T., Henn, R. and Sharma, S.D. (2002). Wash waves generated by ships moving on fairways of varying topography, In: *Twenty-Fourth Symposium on Naval Hydrodynamics 2002*, Fukuoka, Japan.

Kelpšaite, L., Parnell, K.E. and Soomere, T. (2009). Energy pollution: the relative influence of wind-wave and vessel-wake energy in tallinn bay, the baltic sea. *Journal of Coastal Research*, 812–816. ISSN 0749-0208.

Kim, J., Kim, K.S., Kim, Y.C., Van, S.H. and Kim, H.C. (2011). Comparison of potential and viscous methods for the nonlinear ship wave problem. *International Journal of Naval Architecture and Ocean Engineering*, **3**(3), 159–173. ISSN 2092-6782. doi:10.3744/JNAOE.2011.3.3.159.

Kriebel, D. (2007). Mooring loads due to parallel passing ships, In: W. Watson (Editor), *The Proceedings of Ports 2007*, American Society of Civil Engineers, Reston, Va.

Kriebel, D. and Seelig, W. (2002). A unified description of ship-generated waves, In: *The Proceedings of Solving Coastal Conundrums*, Thomas Telford Publishing.

Kucera-Hirzinger, V., Schludermann, E., Zornig, H., Weissenbacher, A., Schabuss, M. and Schiemer, F. (2009). Potential effects of navigation-induced wave wash on the early life history stages of riverine fish. *Aquatic Sciences*, **71**(1), 94–102. ISSN 1420-9055. doi:10.1007/s00027-008-8110-5.

Kunz (1977). Die wirkung von schiffswellen auf entwässerungsbauwerke: Mitteilungshefte des ludwig-franzius instituts: Bericht nr. 46.

Kurdistani, S.M., Tomasicchio, G.R., D'Alessandro, F. and Hassanabadi, L. (2019). River bank protection from ship-induced waves and river flow. *Water Science and Engineering*, **12**(2), 129–135. ISSN 16742370. doi:10.1016/j.wse.2019.05.002.

Lam, W., Hamil, G.A., Song, Y.C., Robinson, D.J. and Raghunathan, S. (2011). A review of the equations used to predict the velocity distribution within a ship's propeller jet. *Ocean Engineering*, **38**(1), 1–10. ISSN 00298018. doi:10.1016/j.oceaneng.2010.10.016.

Larson, M., Almström, B., Göransson, G., Hanson, H. and Danielsson, P. (2017). Sediment movement induced by ship generated waves in restricted waterways. *Coastal Dynamics 2017*, **120**, 300–311.

Lataire, E., Vantorre, M. and Delefortrie, G. (2012). A prediction method for squat in restricted and unrestricted rectangular fairways. *Ocean Engineering*, **55**, 71–80. ISSN 00298018. doi:10.1016/j.oceaneng.2012.07.009.

Lataire, E., Vantorre, M. and Eloot, K. (2009). Systematic model tests on ship-bank interaction effects, In: K. Eloot and M. Vantorre (Editors), *International conference on Ship manoeuvring in shallow and confined water : bank effects*, 9–22, Royal Institution of Naval Architects.

Lee, B.W. and Lee, C. (2019). Equation for ship wave crests in the entire range of water depths. *Coastal Engineering*, **153**, 103542. ISSN 03783839. doi:10.1016/j.coastaleng.2019.103542.

Lesser, G.R., Roelvink, J.A., van Kester, J. and Stelling, G.S. (2004). Development and validation of a three-dimensional morphological model. *Coastal Engineering*, **51**(8-9), 883–915. ISSN 03783839. doi:10.1016/j.coastaleng.2004.07.014.

Li, Z., Bouscasse, B., Gentaz, L., Ducrozet, G. and Ferrant, P. (2018). Progress in coupling potential wave models and two-phase solvers with the swense methodology, In: *the Proceedings of ASME 2018 37th International Conference on Ocean, Offshore and Arctic Engineering*, American Society of Mechanical Engineers Digital Collection.

Li, Z., Deng, G., Queutey, P., Bouscasse, B., Ducrozet, G., Gentaz, L., Le Touzé, D. and Ferrant, P. (2019). Comparison of wave modeling methods in cfd solvers for ocean engineering applications. *Ocean Engineering*, **188**, 106237. ISSN 00298018. doi:10.1016/j.oceaneng.2019.106237.

Lian, F., Jin, J. and Yang, Z. (2019). Optimal container ship size: a global cost minimization approach. *Maritime Policy & Management*, **46**(7), 802–817. ISSN 0308-8839. doi:10.1080/03088839.2019.1630760.

Liang, D., Liu, H., Tang, H. and Rana, R. (2013). Comparison between boussinesq and shallow-water models in predicting solitary wave runup on plane beaches. *Coastal Engineering Journal*, **55**(4), 1350014–1–1350014–24. ISSN 2166-4250. doi:10.1142/S0578563413500149.

Liedermann, M., Tritthart, M., Gmeiner, P., Hinterleitner, M., Schludermann, E., Keckeis, H. and Habersack, H. (2014). Typification of vessel-induced waves and their interaction with different bank types, including management implications for river restoration projects. *Hydrobiologia*, **729**(1), 17–31. ISSN 0018-8158. doi:10.1007/s10750-014-1829-1.

Linde, F., Ouahsine, A., Huybrechts, N. and Sergent, P. (2017). Three-dimensional numerical simulation of ship resistance in restricted waterways: Effect of ship sinkage and channel restriction. *Journal of Waterway, Port, Coastal, and Ocean Engineering*, **143**(1), 06016003. ISSN 0733-950X. doi:10.1061/(ASCE)WW.1943-5460.0000353.

Liu, P.L.F. and Wu, T.R. (2004). Waves generated by moving pressure disturbances in rectangular and trapezoidal channels. *Journal of Hydraulic Research*, **42**(2), 163–171. ISSN 0022-1686. doi:10.1080/00221686.2004.9628301.

Liu, S., Papanikolaou, A. and Zaraphonitis, G. (2011). Prediction of added resistance of ships in waves. *Ocean Engineering*, **38**(4), 641–650. ISSN 00298018.

Lojek, O., Goseberg, N. and Schlurmann, T. (2021). Projecting hydro-morphodynamic impacts of planned layout changes for a coastal harbor: (forthcoming). *Journal of Waterway, Port, Coastal, and Ocean Engineering*. ISSN 0733-950X.

Lu, X., Chen, Y., Denver John Chandar, D. and Lou, J. (2016). Coupling of viscous and potential flow models with free surface: Implementation and application to offshore engineering. *International Journal of Computational Methods and Experimental Measurements*, **4**(4), 413–423. ISSN 2046-0546. doi:10.2495/CMEM-V4-N4-413-423.

Lungu, A. (2020). Numerical simulation of the squatting of floating bodies moving in shallow water. *Procedia Manufacturing*, **46**, 432–439. ISSN 2351-9789. doi:10.1016/j.promfg.2020.03.063.

Luo, Y., Zhang, C., Liu, J., Xing, H., Zhou, F., Wang, D., Long, X., Wang, S., Wang, W. and Shi, F. (2022). Identifying ship-wakes in a shallow estuary using machine learning. *Ocean Engineering*, **246**, 110456. ISSN 00298018. doi:10.1016/j.oceaneng.2021.110456.

Lv, X., Wu, X., Sun, J. and Tu, H. (2013). Trim optimization of ship by a potential-based panel method. *Advances in Mechanical Engineering*, **5**, 378140. ISSN 1687-8140. doi:10.1155/2013/378140.

Ma, C., Zhu, Y., He, J., Zhang, C., Wan, D., Yang, C. and Noblesse, F. (2018). Nonlinear corrections of linear potential-flow theory of ship waves. *European Journal of Mechanics - B/Fluids*, **67**, 1–14. ISSN 09977546. doi:10.1016/j.euromechflu.2017.07.006.

Macdonald, N.J. (2003). Numerical modelling of coupled drawdown and wake, In: *the proceedings of the Canadian Coastal Conference 2003*.

Macfarlane, G.J., Bose, N. and Duffy, J.T. (2014). Wave wake: Focus on vessel operations within sheltered waterways. *Journal of Ship Production and Design*, **30**(3), 109–125. ISSN 21582866. doi:10.5957/JSPD.30.3.130055.

Madsen, P.A. and Schäfer, H.A. (1999). A review of boussinesq-type equations for surface gravity waves, In: P.L.F. Liu (Editor), *Advances in coastal and ocean engineering*, volume 5, 1–94, World Scientific Pub. Co, Singapore and River Edge, N.J.

Mallidis, I., Iakovou, E., Dekker, R. and Vlachos, D. (2018). The impact of slow steaming on the carriers' and shippers' costs: The case of a global logistics network. *Transportation Research Part E: Logistics and Transportation Review*, **111**, 18–39. ISSN 13665545. doi:10.1016/j.tre.2017.12.008.

Mao, L. and Chen, Y. (2020). Investigation of ship-induced hydrodynamics and sediment suspension in a heavy shipping traffic waterway. *Journal of Marine Science and Engineering*, **8**(6), 424. doi:10.3390/jmse8060424.

Marine Insight (2021). Top 10 world's largest container ships in 2021: https://www.marineinsight.com/know-more/top-10-worlds-largest-container-ships-in-2019/.

Matheja, A. and Schweter, L. (2007). Field measurements for the determination of ship-induced loads in a tidal river port: Mitteilungshefte des ludwig-franzius instituts 95: https://www.lufi.uni-hannover.de/fileadmin/lufi/Franzius-Mitteilungen/heft95_artikel02.pdf.

Maynord, S. (1996). Return velocity and drawdown in navigable waterways: Usace technical report: https://apps.dtic.mil/sti/pdfs/ADA286906.pdf.

Maynord, S. (2003). Ship effects before and after deepening of sabine-neches waterway, port arthur, texas: Usace technical report: https://apps.dtic.mil/sti/citations/ADA417939.

Maynord, S. (2004). Ship effects at the bankline of navigation channels. *Proceedings of the Institution of Civil Engineers - Maritime Engineering*, **157**(2), 93–100. ISSN 1741-7597. doi:10.1680/maen.2004.157.2.93.

Maynord, S.T. (2005). Wave height from planing and semi-planing small boats. *River Research and Applications*, **21**(1), 1–17. ISSN 1535-1459. doi:10.1002/rra.803.

McTaggart, K. (2018). Ship squat prediction using a potential flow rankine source method. *Ocean Engineering*, **148**, 234–246. ISSN 00298018. doi:10.1016/j.oceaneng.2017.10.016.

Melling, G., Jansch, H., Kondziella, B., Uliczka, K. and Gätje, B. (2019). Damage to rock groynes from long-period ship waves: Towards a probabilistic design method, In: N. Goseberg and T. Schlurmann (Editors), *the proceedings of Coastal Structures 2019, Hannover*.

Melling, G., Jansch, H., Kondziella, B., Uliczka, K. and Gätje, B. (2020). Evaluation of optimised groyne designs in response to long-period ship wave loads at juelssand in the lower elbe estuary: 28. *Die Küste*, **89**. doi:10.18171/1.089103.

Michell, J.H. (1898). Xi. the wave-resistance of a ship. *The London, Edinburgh, and Dublin Philosophical Magazine and Journal of Science*, **45**(272), 106–123. ISSN 1941-5982. doi:10.1080/14786449808621111.

Millward, A. (1996). A review of the prediction of squat in shallow water. *The Journal of Navigation*, **49**(1), 77–88. ISSN 0373-4633. doi:10.1017/S0373463300013126.

Mintgen, G.F. (2018). *Coupling of shallow and non-shallow flow solvers - an open source framework*, Ph.d. thesis, Technische Universität München.

Moctar, O.e., Shigunov, V. and Zorn, T. (2012). Duisburg test case: Post-panamax container ship for benchmarking. *Ship Technology Research*, **59**(3), 50–64. doi:10.1179/str.2012.59.3.004.

Morioka, J., Tajima, Y., Yamanaka, Y., Larson, M., Kuriyama, Y., Shimozono, T. and Sato, S. (2020). Numerical modeling of ship wave generation using green's functions based on linear dispersive wave theory. *Coastal Engineering Journal*, **62**(2), 317–335. ISSN 2166-4250. doi:10.1080/21664250.2020.1755794.

Mucha, P., Deng, G., Gourlay, T. and El Moctar, O. (2016). Validation studies on numerical prediction of ship squat and resistance in shallow water, In: Klemens Uliczka, Carl-Uwe Böttner, Marko Kastens, Katrien Eloot, Guillaume Delefortrie, Marc Vantorre, Maxim Candries, Evert Lataire (Editor), *in the proceedings of 4th MASHCON*, Bundesanstalt für Wasserbau, Karlsruhe.

Mucha, P. and Moctar, O.e. (2014). Numerical prediction of resistance and squat for a containership in shallow water, In: *the Proceedings of 17th Numerical Towing Tank Symposium*.

Musiedlak, P.H., Ransley, E.J., Hann, M., Child, B. and Greaves, D.M. (2020). Time-splitting coupling of wavedyn with openfoam by fidelity limit identified from a wec in extreme waves. *Energies*, **13**(13), 3431. ISSN 1996-1073. doi:10.3390/en13133431.

Nascimento, M.F.d., Neves, C.F. and de Freitas Maciel, G. (2009). Propagation of ship waves on a sloping bottom, In: J.M. Smith (Editor), *the Proceedings of the 31th international conference on Coastal Engineering, Hamburg, Germany, 2008*, 696–708, World Scientific, Hackensack, NJ.

Noblesse, F., Huang, F. and Yang, C. (2013). The neumann–michell theory of ship waves. *Journal of Engineering Mathematics*, **79**(1), 51–71. ISSN 0022-0833. doi:10.1007/s10665-012-9568-7.

Oebius, H. (2000). Charakterisierung der einflussgrößen schiffsumströmung und propellerstrahl auf die wasserstraßen. *Mitteilungsblatt der Bundesanstalt für Wasserbau*, **82**, 7–22.

Ohle, N. and Zimmermann, C. (2003). Untersuchungen zu den deckwerksverwerfungen am nordufer der elbe: Mitteilungshefte des ludwig-franzius instituts heft-nr. 89.

Palmer, M.A., Bernhardt, E.S., Allan, J.D., Lake, P.S., Alexander, G., Brooks, J., Carr, J., Clayton, S., Dahm, C.N., Follstad Shah, J., Galat, D.L., Loss, S.G., Goodwin, P., Hart, D.D., Hassett, B., Jenkinson, R., Kondolf, G.M., Lave, R., Meyer, J.L., O'Donnell, T.K., Pagano, L. and Sudduth, E. (2005). Standards for ecologically successful river restoration. *Journal of Applied Ecology*, **42**(2), 208–217. ISSN 1365-2664. doi:10.1111/j.1365-2664.2005.01004.x.

Parchure, T.M., Davis, J.E. and McAdory, R.T. (2007). Modeling fine sediment resuspension due to vessel passage, In: J.Y. Maa, L.P. Sanford and D.H. Schoellhamer (Editors), *Proceedings in Marine Science : Estuarine and Coastal Fine Sediments Dynamics*, volume 8, 449–464, Elsevier.

Park, C., Richardson, H.W. and Park, J. (2020). Widening the panama canal and u.s. ports: historical and economic impact analyses. *Maritime Policy & Management*, **47**(3), 419–433. ISSN 0308-8839. doi:10.1080/03088839.2020.1721583.

Park, N.K. and Suh, S.C. (2019). Tendency toward mega containerships and the constraints of container terminals. *Journal of Marine Science and Engineering*, **7**(5), 131. doi:10.3390/jmse7050131.

Parnell, K.E., Soomere, T., Zaggia, L., Rodin, A., Lorenzetti, G., Rapaglia, J. and Scarpa, G.M. (2015). Ship-induced solitary riemann waves of depression in venice lagoon. *Physics Letters A*, **379**(6), 555–559. ISSN 03759601. doi:10.1016/j.physleta.2014.12.004.

Paulsen, B.T., Bredmose, H. and Bingham, H.B. (2014). An efficient domain decomposition strategy for wave loads on surface piercing circular cylinders: Coastal engineering, 86, 57-76. *Coastal Engineering*, **86**, 57–76. ISSN 03783839. doi:10.1016/J.COASTALENG.2014.01.006.

Pawar, R., Bhar, A. and Dhavalikar, S.S. (2019). Numerical prediction of hydrodynamic forces on a moored ship due to a passing ship. *Proceedings of the Institution of Mechanical Engineers, Part M: Journal of Engineering for the Maritime Environment*, **233**(2), 575–585. ISSN 2041-3084. doi:10.1177/1475090218770039.

Pearson, W.H. and Skalski, J.R. (2011). Factors affecting stranding of juvenile salmonids by wakes from ship passage in the lower columbia river. *River Research and Applications*, **27**(7), 926–936. ISSN 1535-1459. doi:10.1002/rra.1397.

Peng, H., Ni, S. and Qiu, W. (2014). Wave pattern and resistance prediction for ships of full form. *Ocean Engineering*, **87**, 162–173. ISSN 00298018. doi:10.1016/j.oceaneng.2014.06.004.

Pethiyagoda, R., Moroney, T.J., Macfarlane, G.J., Binns, J.R. and McCue, S.W. (2018). Time-frequency analysis of ship wave patterns in shallow water: modelling and experiments. *Ocean Engineering*, **158**, 123–131. ISSN 00298018. doi:10.1016/j.oceaneng.2018.01.108.

Plate, U. and Keil, G.W. (1971). Sediment-transport in einem seeschifffahrtskanal. *Die Küste*, **21**, 59–60.

Rapaglia, J., Zaggia, L., Ricklefs, K., Gelinas, M. and Bokuniewicz, H. (2011). Characteristics of ships' depression waves and associated sediment resuspension in venice lagoon, italy. *Journal of Marine Systems*, **85**(1-2), 45–56. ISSN 09247963. doi:10.1016/j.jmarsys.2010.11.005.

Ravens, T.M. and Thomas, R.C. (2008). Ship wave-induced sedimentation of a tidal creek in galveston bay. *Journal of Waterway, Port, Coastal, and Ocean Engineering*, **134**(1), 21–29. ISSN 0733-950X. doi:10.1061/(ASCE)0733-950X(2008)134:1(21).

Rodin, A., Soomere, T., Parnell, K.E. and Zaggia, L. (2015). Numerical simulation of the propagation of ship-induced riemann waves of depression into the venice lagoon. *Proceedings of the Estonian Academy of Sciences*, **64**(1), 22. ISSN 1736-6046. doi:10.3176/proc.2015.1.04.

Rodrigues, S., Santos, J.A. and Soares, C.G. (2018). Numerical and experimental study of ship-generated waves, In: C.G. Soares and T.A. Santos (Editors), *the Proceedings of the 4th International Conference on Maritime Tecnology and Engineering, MARTECH 2018, Lisbon, Portugal*.

Roeber, V. and Cheung, K.F. (2012). Boussinesq-type model for energetic breaking waves in fringing reef environments. *Coastal Engineering*, **70**, 1–20. ISSN 03783839. doi:10.1016/j.coastaleng.2012.06.001.

Russell, J.S. (1845). *Report on Waves: Made to the Meetings of the British Association in 1842-43*, Richard and John E. Taylor, London.

Samaras, A.G. and Karambas, T.V. (2021). Numerical simulation of ship-borne waves using a 2dh post-boussinesq model. *Applied Mathematical Modelling*, **89**, 1547–1556. ISSN 0307904X. doi:10.1016/j.apm.2020.08.034.

Scarpa, G.M., Zaggia, L., Manfè, G., Lorenzetti, G., Parnell, K., Soomere, T., Rapaglia, J. and Molinaroli, E. (2019). The effects of ship wakes in the venice lagoon and implications for the sustainability of shipping in coastal waters. *Scientific Reports*, **9**(1), 19014. ISSN 2045-2322. doi:10.1038/s41598-019-55238-z.

Schijf, J.B. (1949). Protection of embankments and bed in inland and maritime waters, and in overflows or weirs. *PIANC 17th congress 1949, Lisbon, section SI C2*.

Schludermann, E., Liedermann, M., Hoyer, H., Tritthart, M., Habersack, H. and Keckeis, H. (2014). Effects of vessel-induced waves on the yoy-fish assemblage at two different habitat types in the main stem of a large river (danube, austria). *Hydrobiologia*, **729**(1), 3–15. ISSN 0018-8158. doi:10.1007/s10750-013-1680-9.

Schoellhamer, D.H. (1996). Anthropogenic sediment resuspension mechanisms in a shallow microtidal estuary. *Estuarine, Coastal and Shelf Science*, **43**(5), 533–548. ISSN 0272-7714. doi:10.1006/ecss.1996.0086.

Schroevers, M., Huisman, B., van der Wal, M. and Terwindt, J. (2011). Measuring ship induced waves and currents on a tidal flat in the western scheldt estuary, In: J. Rizoli White (Editor), *Proceedings of 2011 IEEE/OES 10th current, waves and turbulence measurements (CWTM 2011)*, 123–129, IEEE, Piscataway, NJ.

Shahjada Tarafder, M. and Suzuki, K. (2008). Numerical calculation of free-surface potential flow around a ship using the modified rankine source panel method. *Ocean Engineering*, **35**(5-6), 536–544. ISSN 00298018. doi:10.1016/j.oceaneng.2007.11.004.

Shi, F., Kirby, J.T., Harris, J.C., Geiman, J.D. and Grilli, S.T. (2012). A high-order adaptive time-stepping tvd solver for boussinesq modeling of breaking waves and coastal inundation. *Ocean Modelling*, **43-44**, 36–51. ISSN 1463-5003. doi:10.1016/j.ocemod.2011.12.004.

Shuster, R., Sherman, D.J., Lorang, M.S., Ellis, J.T. and Hopf, F. (2020). Erosive potential of recreational boat wakes. *Journal of Coastal Research*, **Special Issue No. 95**, 1279–1283. ISSN 0749-0208. doi:10.2112/SI95-247.1.

Silinski, A., Heuner, M., Schoelynck, J., Puijalon, S., Schröder, U., Fuchs, E., Troch, P., Bouma, T.J., Meire, P. and Temmerman, S. (2015). Effects of wind waves versus ship waves on tidal marsh plants: a flume study on different life stages of scirpus maritimus. *PLOS ONE*, **10**(3), e0118687. ISSN 1932-6203. doi:10.1371/journal.pone.0118687.

Smit, P., Zijlema, M. and Stelling, G. (2013). Depth-induced wave breaking in a non-hydrostatic, near-shore wave model. *Coastal Engineering*, **76**, 1–16. ISSN 03783839. doi:10.1016/j.coastaleng.2013.01.008.

Söhngen, B., Fleischer, P. and Liebenstein, H. (2018). German guidelines for designing alternative bank protection measures. *Journal of Applied Water Engineering and Research*, **6**(4), 298–305. doi:10.1080/23249676.2018.1514281.

Soomere, T. (2005). Fast ferry traffic as a qualitatively new forcing factor of environmental processes in non-tidal sea areas: A case study in tallinn bay, baltic sea. *Environmental Fluid Mechanics*, **5**(4), 293–323. ISSN 1573-1510. doi:10.1007/s10652-005-5226-1.

Soomere, T. (2007). Nonlinear components of ship wake waves. *Applied Mechanics Reviews*, **60**(3), 120–138. ISSN 0003-6900. doi:10.1115/1.2730847.

Sorensen, R.M. (1997). Prediction of vessel-generated waves with reference to vessels common to the upper mississippi river system: Usace technical report: https://www.semanticscholar.org/paper/Prediction-of-vessel-generated-waves-with-reference-Sorensen/6ea749e2817a7e9d262e30ba3b5d07a9554a7f1b.

South Carolina Ports Authority (2021). Harbor deepening: https://scspa.com/facilities/port-expansion/harbor-deepening/: last access: 1.2.2022.

Stastistisches Bundesamt (2018). Schiffsankünfte: Bundesländer mit seehäfen, jahre,schiffsart, bruttoraumzahlklasse: https://www.govdata.de/suchen/-/details/schiffsankunfte-bundeslander-mit-seehafen-jahreschiffsart-bruttoraumzahlklasse.

Stelling, G. and Zijlema, M. (2003). An accurate and efficient finite-difference algorithm for non-hydrostatic free-surface flow with application to wave propagation. *International Journal for Numerical Methods in Fluids*, **43**(1), 1–23. ISSN 0271-2091. doi:10.1002/fld.595.

Stern, F., Yang, J., Wang, Z., Sadat-Hosseini, H., Mousaviraad, M., Bhushan, S. and Xing, T. (2013). Computational ship hydrodynamics: Nowadays and way forward. *International Shipbuilding Progress*, **60**(1-4), 3–105. ISSN 0020-868X. doi:10.3233/ISP-130090.

Stockstill, R.L. and Berger, R.C. (2001). Simulating barge drawdown and currents in channel and backwater areas. *Journal of Waterway, Port, Coastal, and Ocean Engineering*, **127**(5), 290–298. ISSN 0733-950X. doi:10.1061/(ASCE)0733-950X(2001)127:5(290).

Styles, R. and Hartman, M.A. (2019). Effect of tidal stage on sediment concentrations and turbulence by vessel wake in a coastal plain saltmarsh. *Journal of Marine Science and Engineering*, **7**(6), 192. doi:10.3390/jmse7060192.

Symmank, L., Natho, S., Scholz, M., Schröder, U., Raupach, K. and Schulz-Zunkel, C. (2020). The impact of bioengineering techniques for riverbank protection on ecosystem services of riparian zones. *Ecological Engineering*, **158**, 106040. ISSN 09258574. doi:10.1016/j.ecoleng.2020.106040.

Taylor, D., Hall, K. and Macdonald, N. (2007). Investigations into ship induced hydrodynamics and scour in confined shipping channels, In: C. Lemckert (Editor), *the Proceedings of the 9th International Coastal Symposium, Queensland, Australia,*, Journal of Coastal Research.

Terziev, M., Tezdogan, T. and Incecik, A. (2020). Modelling the hydrodynamic effect of abrupt water depth changes on a ship travelling in restricted waters using cfd. *Ships and Offshore Structures*, 1–17. ISSN 1744-5302. doi:10.1080/17445302.2020.1816731.

Terziev, M., Tezdogan, T. and Incecik, A. (2022). Scale effects and full-scale ship hydrodynamics: A review. *Ocean Engineering*, **245**, 110496. ISSN 00298018. doi:10.1016/j.oceaneng.2021.110496.

Terziev, M., Tezdogan, T., Oguz, E., Gourlay, T., Demirel, Y.K. and Incecik, A. (2018). Numerical investigation of the behaviour and performance of ships advancing through restricted shallow waters. *Journal of Fluids and Structures*, **76**, 185–215. ISSN 08899746. doi:10.1016/j.jfluidstructs.2017.10.003.

Tezdogan, T., Incecik, A. and Turan, O. (2016). A numerical investigation of the squat and resistance of ships advancing through a canal using cfd. *Journal of Marine Science and Technology*, **21**(1), 86–101. ISSN 0948-4280. doi:10.1007/s00773-015-0334-1.

Thomson, W. (1887). On ship waves: Proceedings of the institution of mechanical engineers, 38(1), 409-434. *Proceedings of the Institution of Mechanical Engineers*, **38**(1), 409–434. ISSN 0020-3483.

Torsvik, T., Pedersen, G. and Dysthe, K. (2009). Waves generated by a pressure disturbance moving in a channel with a variable cross-sectional topography. *Journal of Waterway, Port, Coastal, and Ocean Engineering*, **135**(3), 120–123. ISSN 0733-950X.

Torsvik, T. and Soomere, T. (2008). Simulation of patterns of wakes from high-speed ferries in tallinn bay. *Estonian Journal of Engineering*, **57**(3), 232. ISSN 1736-6038. doi:10.3176/eng.2008.3.04.

Tuck, E.O. (1965). Shallow water flows past slender bodies. *David W. Taylor Model Basin, Washington DC, Published in: Journal of Fluid Mechanics, Volume 26, 1965, pp. 81-95.*

Tuck, E.O. (1967). Sinkage and trim in shallow water of finite width. *David W. Taylor Model Basin, Washington DC, Published in: Zeitschrift Schiffstechnik, Band 14, Heft 73, 1967, pp. 92-94.*

Uliczka, C. and Kondziella, B. (2006). Fahrrinnenanpassung der unterweser an die entwicklungen im schiffsverkehr: Baw - technical reports: http://www.weseranpassung.de/downloads/dateien/Planfeststellungsunterlagen/Unterweser/I.4_UW_Schiffsbelastungen_2006_03_24.pdf.

Uliczka, C. and Walte, C. (1996). Anpassung der fahrrinne der unter- und außenelbe an die containerschifffahrt - ausbaubedingte änderungen der schiffserzeugten belastungen: Baw - technical reports: https://www.kuestendaten.de/media/zdm/portaltideelbe/Projekte/FRA1999/Antragsunterlagen/UVU/Materialbestaende/Bereichsauswahl_Band_I/Texte_Band_I/Gutachten_Schiffsbelasteungen_UVU95.pdf.

Uliczka, K., Peters, K. and Fittschen, T. (2009). Ship-induced tide gate load on the lower river weser and lower river elbe, In: J.M. Smith (Editor), *the Proceedings of the 31th international conference on Coastal Engineering, Hamburg, Germany, 2008*, 774–786, World Scientific, Hackensack, NJ.

Ulm, M., Niehüser, S., Kondziella, B., Arns, A., Jensen, J. and Uliczka, K. (2020). Field measurements in the kiel canal, germany: Ship waves, drawdown, and sediment transport. *Journal of Waterway, Port, Coastal, and Ocean Engineering*, **146**(4), 04020020. ISSN 0733-950X. doi:10.1061/(ASCE)WW.1943-5460.0000577.

UNCTAD (2020). Review of maritime transport 2020: United nations conference on trade and development: https://unctad.org/system/files/official-document/rmt2020_en.pdf.

U.S. Army Corps of Engineers (2019). Fact sheet - new york and new jersey harbor deepening: https://www.nan.usace.army.mil/Media/Fact-Sheets/Fact-Sheet-Article-View/Article/487407/fact-sheet-new-york-new-jersey-harbor-50-ft-deepening/.

Vantorre, M., Verzhbitskaya, E. and Laforce, E. (2002). Model test based formulations of ship-ship interaction forces. *Ship Technology Research*, **49**, 124–141.

Verbrugghe, T., Domínguez, J.M., Crespo, A.J., Altomare, C., Stratigaki, V., Troch, P. and Kortenhaus, A. (2018). Coupling methodology for smoothed particle hydrodynamics modelling of non-linear wave-structure interactions. *Coastal Engineering*, **138**, 184–198. ISSN 03783839. doi:10.1016/j.coastaleng.2018.04.021.

von Häfen, H., Goseberg, N., Stolle, J. and Nistor, I. (2019). Gate-opening criteria for generating dam-break waves. *Journal of Hydraulic Engineering*, **145**(3), 04019002. ISSN 0733-9429. doi:10.1061/(ASCE)HY.1943-7900.0001567.

Vukcevic, V. (2016). *Numerical Modelling of Coupled Potential and Viscous Flow for Marine Applications*, Ph.D. thesis, University of Zagreb.

Vukčević, V., Jasak, H. and Malenica, Š. (2016). Decomposition model for naval hydrodynamic applications, part i: Computational method. *Ocean Engineering*, **121**, 37–46. ISSN 00298018. doi:10.1016/j.oceaneng.2016.05.022.

Wang, P. and Cheng, J. (2021). Mega-ship-generated tsunami: A field observation in tampa bay, florida. *Journal of Marine Science and Engineering*, **9**(4), 437. doi:10.3390/jmse9040437.

Wang, W., Kamath, A., Martin, T., Pákozdi, C. and Bihs, H. (2020*a*). A comparison of different wave modelling techniques in an open-source hydrodynamic framework. *Journal of Marine Science and Engineering*, **8**(7), 526.

Wang, W., Martin, T., Kamath, A. and Bihs, H. (2020*b*). An improved depth–averaged nonhydrostatic shallow water model with quadratic pressure approximation. *International Journal for Numerical Methods in Fluids*, **92**(8), 803–824. ISSN 0271-2091. doi:10.1002/fld.4807.

Wei, M., Chiew, Y.M. and Cheng, N.S. (2020). Recent advances in understanding propeller jet flow and its impact on scour. *Physics of Fluids*, **32**(10), 101303. ISSN 1070-6631. doi:10.1063/5.0023266.

Wilson, R., Wells, S. and Heber, C. (1978). Powering prediction for surface effect ships based on model results, In: *Advanced Marine Vehicles Conference*, American Institute of Aeronautics and Astronautics, Reston, Virigina.

Wolter, C. and Arlinghaus, R. (2003). Navigation impacts on freshwater fish assemblages: the ecological relevance of swimming performance. *Reviews in Fish Biology and Fisheries*, **13**(1), 63–89. ISSN 09603166. doi:10.1023/A:1026350223459.

Wolter, C., Arlinghaus, R., Sukhodolov, A. and Engelhardt, C. (2004). A model of navigation-induced currents in inland waterways and implications for juvenile fish displacement. *Environmental Management*, **34**(5), 656–668. ISSN 1432-1009. doi:10.1007/s00267-004-0201-z.

WSV (2021*a*). Bedarf und planung - fahrrinnenanpassung unter- und außenelbe: https://www.fahrrinnenanpassung.de/bedarf-und-planung.html: - last access: 1.2.2022.

WSV (2021*b*). Fahrrinnenanpassung elbe - schifffahrt profitiert von weiterer zusätzlicher breite! https://www.gdws.wsv.bund.de/SharedDocs/Pressemitteilungen/DE/20210215_Elbe_PM.html: - last access: 1.2.2022.

Wu, T.Y.T. (1987). Generation of upstream advancing solitons by moving disturbances. *Journal of Fluid Mechanics*, **184**, 75–99. ISSN 1469-7645. doi:10.1017/S0022112087002817.

Yao, J.x. and Zou, Z.j. (2010). Calculation of ship squat in restricted waterways by using a 3d panel method. *Journal of Hydrodynamics*, **22**(S1), 472–477. ISSN 1001-6058. doi:10.1016/S1001-6058(09)60241-9.

Yuan, Y., Shi, F., Kirby, J.T. and Yu, F. (2020). Funwave–gpu: Multiple–gpu acceleration of a boussinesq–type wave model. *Journal of Advances in Modeling Earth Systems*, **12**(5). ISSN 1942-2466. doi:10.1029/2019MS001957.

Zaggia, L., Lorenzetti, G., Manfé, G., Scarpa, G.M., Molinaroli, E., Parnell, K.E., Rapaglia, J.P., Gionta, M. and Soomere, T. (2017). Fast shoreline erosion induced by ship wakes in a coastal lagoon: Field evidence and remote sensing analysis. *PLOS ONE*, **12**(10), e0187210. ISSN 1932-6203. doi:10.1371/journal.pone.0187210.

Zeng, Q., Hekkenberg, R., Thill, C. and Hopman, H. (2020). Scale effects on the wave-making resistance of ships sailing in shallow water. *Ocean Engineering*, **212**, 107654. ISSN 00298018. doi:10.1016/j.oceaneng.2020.107654.

Zhang, X., Simons, R., Zheng, J. and Zhang, C. (2022). A review of the state of research on wave-current interaction in nearshore areas. *Ocean Engineering*, **243**, 110202. ISSN 00298018. doi:10.1016/j.oceaneng.2021.110202.

Zhang, X.s., Wang, J.h. and Wan, D.c. (2020). Numerical techniques for coupling hydrodynamic problems in ship and ocean engineering. *Journal of Hydrodynamics*, **32**(2), 212–233. ISSN 1001-6058. doi:10.1007/s42241-020-0021-5.

Zhou, M., Roelvink, D., Verheij, H. and Ligteringen, H. (2013). Study of passing ship effects along a bank by delft3d-flow and xbeach, In: *the Proceedings of International Workshop on Nautical Traffic Models 2013, Delft, the netherlands*.

Zijlema, M. (2020). Computation of free surface waves in coastal waters with swash on unstructured grids. *Computers & Fluids*, **213**, 104751. ISSN 00457930. doi:10.1016/j.compfluid.2020.104751.

Zou, L. and Larsson, L. (2013*a*). Computational fluid dynamics (cfd) prediction of bank effects including verification and validation. *Journal of Marine Science and Technology*, **18**(3), 310–323. ISSN 0948-4280. doi:10.1007/s00773-012-0209-7.

Zou, L. and Larsson, L. (2013*b*). Numerical predictions of ship-to-ship interaction in shallow water. *Ocean Engineering*, **72**, 386–402. ISSN 00298018. doi:10.1016/j.oceaneng.2013.06.015.